Confining strings in SU(N) gauge theories

B. Lucini and M. Teper

Theoretical Physics, University of Oxford, 1 Keble Road, Oxford OX1 3NP, UK

Abstract

We calculate the string tensions of k-strings in SU(N) gauge theories in both 3 and 4 dimensions. We do so for SU(4) and SU(5) in D=3+1, and for SU(4) and SU(6) in D=2+1. In D=3+1, we find that the ratio of the $k = 2$ string tension to the $k = 1$ fundamental string tension is consistent, within quite small errors, with both the M(-theory)QCD-inspired conjecture that $\sigma_k \propto \sin(\pi k/N)$ and with 'Casimir scaling', $\sigma_k \propto k(N-k)$. In D=2+1, where our results are very precise, we see a definite deviation from the MQCD formula, as well as a much smaller but still significant deviation from Casimir scaling. We find that in both D=2+1 and D=3+1 the high temperature spatial k-string tensions also satisfy approximate Casimir scaling. We point out that approximate Casimir scaling arises naturally if the cross-section of the flux tube is nearly independent of the flux carried, and that this will occur in an effective dual superconducting description, if we are in the deep-London limit. We estimate, numerically, the intrinsic width of k-strings in D=2+1 and indeed find little variation with k. In addition to the stable k-strings we investigate some of the unstable strings, which show up as resonant states in the string mass spectrum. While in D=3+1 our results are not accurate enough to extract the string tensions of unstable strings, our more precise calculations in D=2+1 show that there the ratios between tensions of unstable strings and the tension of the fundamental string are in reasonably agreement with (approximate) Casimir scaling. We also investigate the basic assumption that confining flux tubes are described by an effective string theory at large distances, and attempt to determine the corresponding universality class. We estimate the coefficient of the universal Lüscher correction from periodic strings that are longer than 1 fermi, and find $c_L = 0.98(6)$ in D=3+1 and $c_L = 0.560(24)$ in D=2+1. These values are consistent with a simple bosonic string, $c_L = \pi/3$ and $c_L = \pi/6$ respectively, and are inconsistent with other simple effective string theories such as fermionic, supersymmetric or Neveu-Schwartz.

PACS Numbers: 11.15.-q, 12.38.Aw, 11.15.Ha, 12.39.Pn.
Key Words: SU(N) Gauge Theories, Lattice Gauge Theories, Confinement, String Tension, Strings in Higher Representations.

1 Introduction

It is widely believed that the SU(3) gauge theory that underlies QCD is linearly confining and that this explains why we do not observe quarks (or gluons) in nature. The fact that confinement is linear suggests that the colour-electric flux between fundamental charges is localised in a tube between those charges and it is attractive to think that the long-distance physics of such flux tubes is given by an effective string theory. The simplest possibility is that this string theory is bosonic but other possibilities are not excluded and indeed might be natural if QCD is obtained by some kind of reduction from a higher-dimensional theory.

The same comments apply to SU(N) gauge theories for $N \neq 3$. Indeed there are long-standing ideas that for $N \to \infty$ the SU(N) gauge theory can be thought of as a string theory. Moreover SU(N) gauge theories in D=2+1 also appear to be linearly confining [1] and all the above comments will apply there as well.

In addition to charges in the fundamental representation (like quarks) one can consider the potential between static charges in higher representations of the gauge group. In SU(2) and SU(3) any such charge can be screened by gluons either to the fundamental or to the trivial representation. Since virtual gluons are always present in the vacuum this means that such a potential will, at large distances, either rise linearly with a string tension equal to the fundamental one or will flatten off to some constant value. (This assumes that the fundamental string tension is the lowest, as appears to be the case.) For $N \geq 4$, however, this is no longer the case and there are new stable strings with string tensions different from the fundamental one. A typical source may be thought of as k fundamental charges located at a point. The confining string is then usually referred to as a k-string. For SU(N) we have non-trivial stable k-strings up to a maximum value of k given by the integer part of $N/2$.

Such k-strings are interesting for a variety of reasons. The values of their string tensions, σ_k, will constrain models of confinement. In models of glueballs in which the latter consist of open or closed strings, the SU(N) mass spectrum should change with N in a way that is determined by how σ_k varies with N and k. In addition there are theoretical ideas concerning the value of σ_k. In particular there is a conjecture based on M-theory approaches to QCD (MQCD) [2] that suggests $\sigma_k \propto \sin\{\pi k/N\}$. One can contrast this with the old "Casimir scaling" conjecture [3] that would suggest $\sigma_k \propto k(N-k)$ and also with the simple possibility that a k-string consists of k non-interacting fundamental strings, in which case $\sigma_k = k\sigma$.

In a string theory the mass of a flux tube of length l will receive a leading large-l correction that is $O(1/l)$. Such a slowly decreasing correction cannot be made negligible simply by making $l \gg 1$fm and so it will, in principle, limit the accuracy of our calculations of σ_k. Fortunately this leading string correction is known to be universal [4] in that its coefficient is determined entirely by the central charge of the effective string theory. The universality class is usually thought to be that of a simple Nambu-Goto bosonic string. There is however no strong direct (numerical) evidence for this

belief that we are aware of. Such evidence would need to be obtained from strings that are longer than 1 fm and to achieve the required accuracy for such strings is a hard numerical problem. Where accurate values are quoted in the literature they typically involve fitting potentials down to shorter distances, where the fits are almost certainly dominated by the tail of the Coulomb term which has the same functional form as the string correction (and in practice a similar coefficient). We have therefore attempted to provide a usefully accurate calculation of this string correction in SU(2) gauge theory, in both D=3+1 and D=2+1. Such a calculation also addresses the fundamental question of whether a confining flux tube is in fact described by an effective string theory at large distances.

The contents of this paper are as follows. In the next Section we describe how we calculate σ_k from the mass of a flux loop that winds around the spatial torus. We contrast this method with one that uses explicit sources; in particular with respect to 'strings' that can break. All this requires a classification of strings in all possible representations of the gauge group (the details of which appear in Section A.1 of the Appendix). In the following Section we summarise the lattice aspects of our calculation; we can be brief since it is entirely standard. We then turn to the basic question of whether we really do have strings and, if so, which universality class they belong to. Confining ourselves to flux tubes that are longer than 1fm we find that in both D=3+1 and D=2+1 SU(2) gauge theory the leading correction to the linear dependence of the string mass is consistent, within quite small errors, with what one expects from the simplest effective bosonic string theory and excludes the most obvious alternatives. We then turn to our calculation of k-strings. We begin by briefly summarising some of the theoretical expectations: MQCD, Euclidean and Hamiltonian (lattice) strong coupling, Casimir scaling, the bag model and simple flux counting. We then turn to our D=3+1 calculations of $\sigma_{k=2}$ in both SU(4) and SU(5) gauge theories and follow this with our (inevitably) much more accurate D=2+1 calculations for SU(4) and SU(6). (In SU(6) we are able to address non-trivial $k = 3$ strings.) In D=3+1 we find consistency with both MQCD and Casimir scaling. In D=2+1 the string tension ratios, while still close to the MQCD formula, are much closer to Casimir scaling. We point out that if the flux is homogeneous, then (approximate) Casimir scaling arises if the flux tube width is (approximately) independent of k. (And, more theoretically, that this will arise in the deep-London limit of a dual superconducting vacuum.) To test this idea we perform an explicit calculation of the intrinsic size of k-strings in D=2+1. We find that the k-string width is indeed largely independent of k, albeit with some interesting if weak differences. We then point out that the same calculations can be reinterpreted as telling us that the spatial string tension in the high temperature deconfining phase satisfies approximate Casimir scaling. We complement this with an explicit D=3+1 high-T calculation that demonstrates that in that case too the string tension ratio is close to Casimir scaling. We then attempt to see if there is any sign of other, unstable, strings, which should appear as excited states in the string mass spectrum. We find reasonably

convincing evidence for such strings, satisfying approximate Casimir scaling, in our D=2+1 calculations. We finish with a discussion of our results and some of their implications.

The D=3+1 SU(4) calculations of $\sigma_{k=2}/\sigma$, as well as a preliminary version of our SU(5) calculations, have appeared in [5]. In the introduction to a recent companion paper on the mass spectrum and topological properties of D=3+1 SU(N) gauge theories [6] we briefly summarised some of our results on σ_k/σ. In particular we drew attention to the relevance of these results on k-strings for the Casimir scaling hypothesis. We remark that all these calculations are intended as a first step to a much more complete and accurate calculation of the properties of SU(N) gauge theories for all values of N.

2 Strings and string breaking

Consider a static source in some representation $\mathcal{R}$ of the gauge group in, say, 3+1 dimensions. Suppose we have a conjugate source a distance r away. If r is small then the potential energy will be dominated by the Coulomb term

$$V_{\mathcal{R}}(r) \stackrel{r\to 0}{=} \frac{C_{\mathcal{R}}\alpha_s(r)}{r} + \dots \tag{1}$$

where $\alpha_s(r)$ is the usual running coupling and $C_{\mathcal{R}}$ is the quadratic Casimir of the representation $\mathcal{R}$:

$$C_{\mathcal{R}} \equiv Tr_{\mathcal{R}} T^a T^a \tag{2}$$

with the T^a being the generators of the group. If the theory is linearly confining, and if we ignore the fact that the source may be screened by gluons, then at large r we expect the potential energy to be given by

$$V_{\mathcal{R}}(r) \stackrel{r\to\infty}{=} \sigma_{\mathcal{R}} r - \frac{\pi(D-2)}{24}\frac{c_s}{r} + \dots . \tag{3}$$

Here $\sigma_{\mathcal{R}}$ is the 'string tension' of the confining flux tube joining the sources and how its value varies with the representation $\mathcal{R}$ is an interesting physical question. If the long-distance physics of the confining flux tube is described by an effective string theory, then the $O(1/r)$ correction in eqn(3) is the Casimir energy of a string with fixed ends, and c_s is proportional to the central charge. This correction is universal [4], since it depends only upon the massless modes in the effective string theory and does not depend upon the detailed and complicated dynamics of the flux tube on scales comparable to its width. The central charge is given [7] by the number of massless bosonic and fermionic modes that propagate along the string. In practice it is usually assumed that $c_s = 1$, corresponding to the simplest possible (Nambu-Goto) bosonic string theory. However, these modes are not related to the fundamental degrees of freedom of our SU(N)

gauge theory in any transparent way and the presence of fermionic modes is certainly not excluded. For example, we have the following simple possibilities [8]:

$$c_s = \begin{cases} 1 & \text{bosonic} \\ \frac{1}{4} & \text{fermionic} \\ 0 & \text{supersymmetric} \\ \frac{3}{2} & \text{Neveu} - \text{Schwartz} \end{cases} \tag{4}$$

Whether a string description of the confining flux tube is in fact valid and, if so, what is its universality class, are fundamental questions which are still largely open. The examples in eqn(4) show that one needs to calculate c_s to better than, say, $\pm 15\%$ if one is to usefully resolve different possibilities.

In reality the vacuum contains virtual gluons which can screen the static source, and this will complicate any attempt to calculate $\sigma_{\mathcal{R}}$. When and how this happens will depend on the energetics of the system. Suppose the representation $\mathcal{R}$ can be screened to a different representation $\mathcal{R}'$ by a number of gluons. Such a screened source will acquire an extra mass of, say, ΔM. If the string tension corresponding to $\mathcal{R}'$ is smaller than $\sigma_{\mathcal{R}}$, the screening is certain to become energetically favoured for sufficiently large r, since as $r \to \infty$

$$\Delta M \ll V_{\mathcal{R}}(r) - V_{\mathcal{R}'}(r) \simeq \sigma_{\mathcal{R}} r - \sigma_{\mathcal{R}'} r. \tag{5}$$

The minimum value of r at which the energetics favours screening is the string breaking scale r_b. (We shall use the term 'string breaking' when a source is screened to a different representation; even if the latter is not the trivial one.) So if we calculate the potential for our sources we can expect the r-dependence to be given by $V_{\mathcal{R}}(r)$ for $r \leq r_b$ and $V_{\mathcal{R}'}(r)$ for $r \geq r_b$. If r_b is large enough then we will be able to extract $\sigma_{\mathcal{R}}$ from the linearly rising potential at $r \leq r_b$. In practice, however, the string breaking scale is similar to other dynamical scales in the theory and it is not clear whether any apparent linear rise of $V(r)$ for $r \leq r_b$ is due to the precocious formation of a string, from which we can read off $\sigma_{\mathcal{R}}$, or if it is merely accidental. Indeed it may be that one cannot assign an unambiguous meaning to the quantity $\sigma_{\mathcal{R}}$ under these circumstances. However it is also possible that if the string breaking is relatively weak then one may be able to calculate $\sigma_{\mathcal{R}}$ for $r \geq r_b$ by identifying an appropriate excited string state. In any case it is clear that string breaking creates substantial extra ambiguities in any attempt to calculate the properties of strings corresponding to higher representation charges.

For SU(2) and SU(3) any representation $\mathcal{R}$ can be screened by gluons to either the trivial or the fundamental representation. However for SU($N \geq 4$) this is no longer the case and one finds new strings that are completely stable and to which none of the above ambiguities apply. The situation may be summarised as follows. (We leave a fuller discussion to the Appendix.) Suppose the representation $\mathcal{R}$ can be obtained from the product of $n_{\mathcal{R}} + k$ fundamental representations and $n_{\mathcal{R}}$ conjugate ones. Let z be an element of the centre, Z_N, of the SU(N) gauge group. Under such a centre gauge transformation the source will transform as z^k. We shall refer to k as the $\mathcal{N}$-ality of

the representation. Now, since gluons transform trivially under the centre, the source will continue to transform in this way even if it is screened by gluons to some other representation. Thus the same value of k will label a source and all the sources that can be obtained from it by screening. Indeed one can show that if two representations have the same value of k then one can be screened by gluons to the other. Within any given class of such sources there will be a lowest string tension σ_k, which, by string breaking, will provide the potential for any of these sources at large enough distances. The independent values of k are constrained: under charge conjugation $k \to -k$, and we also have $z^k = z^{N-k}$. Thus for SU(N) we have stable strings labelled by $k = 1, ..., k_{max}$ where k_{max} is the integer part of $N/2$ and $k = 1$ is, of course, the fundamental string. That is to say, we must go to at least SU(4) to have a $k = 2$ string, and to at least SU(6) to find a $k = 3$ string.

In this paper we shall compare the $k = 2$ and $k = 1$ string tensions in SU(4) and SU(5) gauge theories in D=3+1. We shall do the same in SU(4) and SU(6) in D=2+1; and in this last case we shall calculate the $k = 3$ string tension as well. In all cases we shall extrapolate to the continuum limit and the aim is to obtain results that are accurate enough to distinguish between various theoretical expectations. Since these strings are all stable there is no intrinsic ambiguity in defining a string tension and we can, in principle, achieve this goal.

We shall calculate σ_k not from the potential between static charges but from the mass of a k-string that winds once around the spatial torus. If the string length l is sufficiently large, its mass will be given by an expression similar to eqn(3):

$$m_k(l) \stackrel{l\to\infty}{=} \sigma_k l - \frac{\pi(D-2)}{6}\frac{c_s}{l} + \dots . \tag{6}$$

We note that because of the different boundary conditions on the ends of the string (periodic rather than fixed) the $O(1/r)$ universal string correction is four times as large as for the static potential [9]. We further note that because there are no explicit sources there is no analogue, at small l, of the Coulomb potential in eqn(1). That is to say, this is a particularly favourable context in which to calculate the string correction: its coefficient is large, and there is no danger of confusing it with a Coulomb interaction which has the same functional form.

One can of course consider such closed but non-contractible winding strings in any representation $\mathcal{R}$. However, just as with the static potential, such a string can be screened to a different string, corresponding to a representation $\mathcal{R}'$, as long as both strings possess the same $\mathcal{N}$-ality. One can picture the string breaking as follows: a pair of gluons pops out of the vacuum somewhere along the string. These then move away from each other along the string. As they do so the section of string between them will no longer belong to $\mathcal{R}$ but rather to the product of $\mathcal{R}$ and the adjoint representation. If the two gluons propagate all the way around the torus they can meet and annihilate leaving a new string that is entirely in this different representation. Clearly one can extend this to any number of gluons. This is just like the breaking of the string between

static sources except that here the gluons eventually annihilate rather than adhering to a source. Thus there is no extra mass ΔM to consider and the breaking can occur for small l if this lowers the mass of the loop. That is to say, there is no region $r \leq r_b$ where one might hope to see a portion of the original string prior to its breaking. Of course, just as for static charges, one might hope to see the unstable string as an excited 'resonant' string in the string mass spectrum.

In addition to the complete string breaking described above, the gluons may propagate only some short distance along the string before returning and annihilating. These virtual processes will renormalise $\sigma_{\mathcal{R}}$, and simple theoretical expectations for the string tension need to take this effect into account.

Since we are considering larger SU(N) groups (partly in order to calculate σ_k for larger k) one immediate question is how this screening will depend on N. In particular we know that particle decay widths vanish in the large-N limit [10]: and it is natural to ask if screening will vanish in a similar way. The answer is yes and no. To appreciate this consider, say, the decay $\rho \to 2\pi$ in large-N QCD. This is suppressed by a factor of $1/N$. However this suppression does not arise from the decay *per se*, but is a consequence of confinement constraining the pions to be colour singlets. If the theory were not confining, so that the 'π'-mesons belonged to the adjoint representation of the colour group, then this decay of the ρ would be unsuppressed once we summed over all the coloured 2π final states. Thus the large-N suppression of particle decays can be thought of as a phase-space suppression due to confinement. In just the same way the process of gluon screening (and renormalisation) of strings will be unsuppressed at large N. However the screening of a string in representation $\mathcal{R}$ to a particular representation $\mathcal{R}'$ in the same $\mathcal{N}$-ality class may be suppressed. Whether it is or is not will depend on the number of states in $\mathcal{R}'$. So, for example, adjoint string breaking, i.e. the adjoint sources being screened by gluons to singlets, will be suppressed as $N \to \infty$. So will be the screening of $k = 1$ strings down to the fundamental and in general the screening of k-strings to the representation with k quarks. (See Appendix A.2 for details.) On the other hand the transformation of the mixed to totally antisymmetric $k = 2$ representations is not suppressed. Of course these general counting arguments should be supplemented by any dynamical information we have. For example we expect $\sigma_k \to k\sigma$ as $N \to \infty$, from the suppression of fluctuations in that limit (and the dominance of a single Master field). This has implications for decays as well.

3 Lattice preliminaries

The way we perform our lattice calculations is entirely standard and follows the pattern described in [6]. For completeness we shall provide a brief summary here.

We shall work on a hypercubic lattice with periodic boundary conditions. The degrees of freedom are SU(N) matrices, U_l, residing on the links, l, of the lattice. In the partition function the fields are weighted with $\exp\{S\}$ where S is the standard

plaquette action

$$S = -\beta \sum_p \Big(1 - \frac{1}{N} ReTr\, U_p \Big), \tag{7}$$

i.e. U_p is the ordered product of the matrices on the boundary of the plaquette p. For smooth fields this action reduces to the usual continuum action with $\beta = 2N/g^2$ in D=3+1 and $\beta = 2N/ag^2$ in D=2+1 (where g^2 has dimensions of mass and the theory is super-renormalisable). By varying the inverse lattice coupling β we vary the lattice spacing a.

The Monte Carlo we use mixes standard heat-bath and over-relaxation steps in the ratio 1 : 4. These are implemented by updating SU(2) subgroups using the Cabibbo-Marinari prescription [11]. We use 3 subgroups in the case of SU(3), 6 for SU(4), 10 for SU(5) and 15 for SU(6). To check that we have enough subgroups for efficient ergodicity we use the same algorithm to minimise the action. We find that with the above number of subgroups, the SU(N) lattice action decreases more-or-less as effectively as it does in the SU(2) gauge theory. We perform calculations of correlation every 5'th such sweep.

We calculate correlations of gauge-invariant operators $\phi(t)$, which depend on field variables within a given time-slice, t. The basic component of such an operator will typically be the (traced) ordered product of the U_l matrices around some closed contour c. A contractible contour, such as the plaquette itself, is used for glueball operators. If, on the other hand, we use a non-contractible closed contour, which winds once around the spatial hyper-torus, then the operator will project onto winding strings of fundamental flux. In the confining phase the theory is invariant under a class of centre gauge transformations that ensure that the overlap between contractible and non-contractible operators is exactly zero, i.e. the string cannot break. For our lattice action the correlation function of such an operator has good positivity properties, i.e. we can write

$$C(t) = \langle \phi^\dagger(t)\phi(0)\rangle = \sum_n |\langle \Omega|\phi|n\rangle|^2 \exp\{-E_n t\} \tag{8}$$

where $|n\rangle$ are the energy eigenstates, with E_n the corresponding energies, and $|\Omega\rangle$ is the vacuum state. If the operator has $\langle\phi\rangle = 0$ then the vacuum will not contribute to this sum and we can extract the mass of the lightest state with the quantum numbers of ϕ, from the large-t exponential decay of $C(t)$. To make the mass calculation more efficient we use operators with definite momentum. (We will often use $\vec{p} = 0$; however, as we will see, when better precision is required, it can be useful to extract extra information from the smallest non-zero momenta.) Note that on a lattice of lattice spacing a we will have $t = an_t$, where n_t is an integer labelling the time-slices, so that what we actually obtain from eqn(8) is aE_n, the energy in lattice units.

In practice a calculation using the simplest lattice string operator is inefficient because the overlap onto the lightest string state is small and so one has to go to large values of t before the contribution of excited states has died away; and at large t the signal has disappeared into the statistical noise. There are standard methods [12] for

curing this problem, using blocked (smeared) link operators and variational techniques. Here we use the simple blocking technique described in detail in [1]. We then have a set of trial operators corresponding to different blocking levels. From the space of operators spanned by these we can determine the best operator using standard variational techniques [1].

Having determined our 'best' operator, we then attempt to fit the corresponding correlation function, normalised so that $C(t = 0) = 1$, with a single exponential in t. (Actually a cosh to take into account the temporal periodicity.) We choose fitting intervals $[t_1, t_2]$ where initially t_1 is chosen to be $t_1 = 0$ and then is increased until an acceptable fit is achieved. The value of t_2 is chosen so that there are at least 3, and preferably 4, values of t being fitted. (Since our fitting function has two parameters.) Where $t_1 = 0$ and the errors on $C(t = a)$ are much smaller than the errors at $t \geq 2a$, this procedure provides no significant evidence for the validity of the exponential fit, and so we use the much larger error from $C(t = 2a)$ rather than $C(t = a)$. (This typically only arises on the coarsest lattices and/or for very massive states.) We ignore correlations between statistical errors at different t and attempt to compensate for this both by demanding a lower χ^2 for the best acceptable fit and by not extending unnecessarily the fitting range. (Although in practice the error on the best fit increases as we increase the fitting range, presumably because the correlation in t of the errors is modest and the decorrelation of the operator correlations is less efficient as t increases.) The relatively rough temporal discretisation of a few of our calculations, means that, at the margins, there are inevitable ambiguities in this procedure. These however decrease as $a \to 0$. Once a fitting range is chosen, the error on the mass is obtained by a jack-knife procedure which deals correctly with any error correlations as long as the binned data are statistically independent. Typically we take 50 bins, each involving between 2000 and 40000 sweeps depending on the calculation. It is plausible that bins of this size are independent; however we have not stored our results in a sufficiently differential form that we can calculate the autocorrelation functions so as to test this in detail. A crude test is provided by recalculating the statistical errors using bins that are twice as large. We find the errors are essentially unchanged when we do so, which provides some evidence for the statistical independence of our original bins.

In addition to the tension of the fundamental $k = 1$ string we also calculate tensions of $k = 2$ and $k = 3$ strings. Denote by P_c the ordered product of the U_l around a non-contractible loop c that winds once around the spatial torus. So TrP_c will project onto a winding loop of fundamental flux. The operators TrP_c^2 and $\{TrP_c\}^2$ will project onto $k = 2$ loops, while the operators TrP_c^3, $TrP_c\{TrP_c\}^2$ and $\{TrP_c\}^3$ will project onto $k = 3$ loops. These operators together with the same ones using blocked links, are summed so as to have $\vec{p} = 0$ and are then used as the basis of our variational calculation for the $k = 2$ and $k = 3$ strings respectively.

4 A universal string correction?

Whether the long-distance dynamics of a confining flux tube is described by an effective string theory and, if so, what is its universality class are fundamental theoretical questions. These are also important practical questions; particularly for an accurate determination of the string tension, since the answer will determine how large is the slowly falling $O(1/l)$ correction to the mass of a long flux tube in eqns(3,6). These are, however, difficult questions to answer numerically requiring, as they do, the accurate calculation of flux tube masses when these are very long and very massive. Thus, although this problem has been addressed many times in the past, the numerical evidence is, as yet, far from convincing. In this Section we shall describe some calculations which aim to improve significantly upon this unsatisfactory situation.

Ideally we would like to perform calculations for the various SU(N) gauge groups that are of interest to us in this paper. In practice our limited computational resources force us to focus upon the SU(2) group. Ideally, again, we would wish to perform calculations for several values of a but again this is not practical. Instead we shall perform calculations at a single value of a which is small enough, $a\sqrt{\sigma} \simeq 0.16$, that we can be confident that we are on the weak-coupling side of any roughening transition. We shall perform such calculations separately for 2+1 and 3+1 dimensions since both cases are of interest and they need not be the same.

When is a string 'long'? Since we expect $\xi_\sigma \equiv 1/\sqrt{\sigma}$ to provide the natural length scale for the physics of the confining flux tube, a string of length $l = aL$ will be long if $l/\xi_\sigma = La\sqrt{\sigma} \gg 1$. We can translate to more familiar physical units by recalling that in the real world $1/\sqrt{\sigma} \simeq 0.45$fm. Since quenched QCD provides a good approximation to QCD, we can, for qualitative purposes, use the same scale in the D=3+1 SU(3) gauge theory. Since it appears that all D=3+1 SU(N) gauge theories are 'close' to each other [6], it should not be too misleading to use the same scale in all cases. For purposes of orientation (and nothing else) we shall also use this scale in $D = 2 + 1$ SU(N) gauge theories (where again all SU(N) gauge theories are 'close' to each other [1]).

4.1 SU(2) in 2+1 dimensions

We perform calculations on L^2L_t lattices at $\beta = 9.0$. (Recall that in $D = 2 + 1$ SU(N) gauge theories [1] the coupling g^2 has dimensions of mass, the theory is super-renormalisible, and $\beta \to 2N/ag^2$ as $a \to 0$.) The flux tube winds around the spatial torus and so has length $l = aL$. We perform calculations for a large number of lattice sizes, ranging from $L = 8$ to $L = 40$. Recall that at this value of β one has $a\sqrt{\sigma} \simeq 0.162$ [1] so that the length of our flux tube ranges from $l = 8a \simeq 1.3\times\xi_\sigma$ to $l = 40a \simeq 6.5\times\xi_\sigma$. In our 'fermi' units the latter translates to $l \simeq 3$fm. This should certainly be long enough to be governed by the long distance effective string dynamics if that indeed provides the correct description.

In addition to the masses, as extracted from the $\vec{p} = 0$ operators, we also calculate

the energies corresponding to the lowest five non-zero momenta transverse to the string: $ap = 2\pi n/L$ for $n = 1, .., 5$. If we want to use these energies to provide extra information on the flux loop mass, care is needed because the continuum energy-momentum dispersion relation, $E^2 = p^2 + m^2$, suffers lattice corrections. To determine these we have fitted the energies on our largest lattices with a more general dispersion relation

$$(aE)^2 = (am)^2 + (ap)^2 + \gamma(ap)^4. \tag{9}$$

We find that for the largest lattices the size of the lattice correction γ is consistent with zero within small errors. For example on the $L = 40$ lattice we obtain $\gamma = 0.06(8)$ for $n \leq 5$. Thus in these cases we can simply set $\gamma = 0$ and use the continuum dispersion relation. For smaller lattices the gap between momenta becomes larger and, not surprisingly, the number of momenta that can be well fitted with $E^2 = p^2 + m^2$ decreases. Since these larger values of E have larger statistical errors there is not much to be gained by attempting to include them and so we simply exclude them from the fits. For the same reason we do not bother with $\vec{p} \neq 0$ for lattices with $L < 20$.

We note that the lattice correction in eqn(9) is $\gamma(ap)^4 = \gamma(2\pi n/L)^4$ and this is of the same order as the higher order non-universal string corrections that we have ignored in eqn(6). We also note that the tree-level lattice dispersion relation provides very bad fits to our calculated energies – it clearly contains lattice corrections that are far too large. Finally we remark that if we generalise eqn(9) so as to allow a renormalisation of the $O(p^2)$ term, we find that the fitted coefficient is unity within very small errors.

We list the masses that we obtain from our $p = 0$ correlators in Table 1. To obtain the values in the first column we have used fits to the correlation functions, $C(t)$, down to the lowest plausible values of t, so as to minimise the errors (which grow with t). In some cases there are indications from the effective masses at larger t that this mass estimate might be optimistic. So we have listed in the second column mass estimates that we regard as very safe, but which might, as a result of being overcautious, overstate the errors and hence weaken the statistical significance of our final fits. Table 1 also contains, in the third column, the mass estimates obtained by using both $p = 0$ and $p \neq 0$ energies in the way described above. Statistically these are the most accurate results, although they run the risk of possessing a small systematic bias from lattice corrections to the continuum energy-momentum dispersion relation. However any such bias will be smallest on the largest lattices and it is only on these that the $p \neq 0$ energies make a significant difference.

An immediately striking feature of the listed masses is that they rise more-or-less linearly with length, all the way out to the longest loops. This demonstrates directly that in D=2+1 SU(2) gauge theories we have linear confinement out to at least $l \sim 3$fm. However this is no more than expected and so we shall not dwell upon it any further here.

We turn now to the real question of interest here: how accurately can we test the $O(1/l)$ string correction term in eqn(6)? As a first step we calculate the effective

value of the coefficient c_s that one obtains from pairs of flux loops of length l and l' respectively:

$$c_s^{eff}(l,l') = \frac{6}{\pi(D-2)} \times \frac{\{\frac{m(l)}{l} - \frac{m(l')}{l'}\}}{\{\frac{1}{l'^2} - \frac{1}{l^2}\}} \tag{10}$$

In Table 2 we list the values of $c_s^{eff}(l,l')$ that one obtains for neighbouring values of l and l' using the masses listed in Table 1. Any given value gives us no information on the validity of the $O(1/l)$ string correction. However if we find that $c_s^{eff}(l,l')$ has a finite non-zero limit as $l, l' \to \infty$ then we will have shown that the leading correction is indeed of this form and the limiting value will provide us with an estimate of the coefficient c_s.

Our most accurate values of c_s^{eff} are those that incorporate $p \neq 0$ energies, and we display these in Fig.1. We see from the plot that for small loop lengths the value of c_s^{eff} is small and increases as the loop length grows. However the behaviour is not monotonic: at intermediate l the value of c_s^{eff} increases through the bosonic string value and perhaps peaks close to the value for a Neveu-Schwartz string. This occurs at a loop size $l \sim 1$fm which is typically the longest loop for which older calculations had usefully accurate results. Thus, by focusing on slightly different intervals close to $l \sim 1$fm it is possible to either confirm or contradict the bosonic string value; but, in either case, incorrectly. To obtain real evidence one must go to longer strings and if one does so, as in Fig.1, one finds that the value of c_s^{eff} decreases again to something that appears consistent with the bosonic string value.

To obtain our estimate of c_s we use eqn(6) to fit all the loop masses that are longer than some reference value l_0. If l_0 is small there is no acceptable fit. As we increase l_0 eventually the fit becomes acceptable. We can then increase l_0 to check the stability of the best fit. In Table 3 we list the results of this procedure for each of our three sets of loop masses. The most accurate values are obtained from the last set, and are plotted in Fig.2. We extract from this our best estimate for the string correction:

$$c_s = 1.070 \pm 0.045. \tag{11}$$

This is close to the bosonic string value and far from that of other simple string theories.

The above analysis assumes that the leading correction to the linear dependence of the mass is $\propto 1/l$. The fact that c_s^{eff} becomes independent, within errors, of l once $l \geq 16a$, tells us that our results are certainly consistent with such a string-like correction. It is interesting to ask how well our calculations exclude other choices. We have therefore performed fits to

$$m(l) = \sigma l + \frac{c}{l^p}. \tag{12}$$

We find that the there are no acceptable fits if any values with $l < 14a$ are included. The fit to $l \geq 14a$ has a mediocre but acceptable χ^2, and we find that the possible range of powers is $p = 1.4 \pm 0.5$. For $l \geq 16a$ the best fit is very good and one finds

$p = 0.9 \pm 0.5$. Fits to $l \geq 20a$ are equally good but no longer provide a useful constraint on p. In short, our results are consistent with the $O(1/l)$ string-like correction term and, in any case, the power of $1/l$ is constrained to be within the range $p = 0.9 \pm 0.5$.

4.2 SU(2) in 3+1 dimensions

We perform calculations on $L^3 L_t$ lattices at $\beta = 2.55$. At this value of β one has $a\sqrt{\sigma} \simeq 0.159$ [6], so that the size of a is very similar to that in our $D = 2 + 1$ calculations. The calculations in D=3+1 are, of course, slower and so our range of lattice sizes and our statistics is somewhat less. One may hope that this will be partly compensated for by the fact that the expected string correction, $(D-2)\pi c_s/6L$, will be twice as large (for a given universality class). We perform calculations on lattices ranging from $L = 8$ to $L = 32$. Thus our longest flux loop is $l = 32a \simeq 2.3$fm which, if our experience in $D = 2 + 1$ is relevant, should be long enough to see the leading correction.

Our calculation and analysis is precisely as in D=2+1, except that the values of the momenta transverse to the flux loop that we use are $p^2 = 0, 1, 2, 4$. The mass estimates are listed in Table 4. As in the D=2+1 case we list two sets of masses extracted from the $p = 0$ correlators. In general our mass estimates are chosen to be those with the smallest errors while still giving plausible fits. In some cases the plausibility is less than convincing and we then also select a 'safer' mass estimate, which will have larger errors. The former numbers provide the first column of masses in Table 4 while the latter provide the second column. The two columns only differ in some cases. The mass estimates obtained using $p \neq 0$ as well as $p = 0$ correlators are also divided into two sets. (A division that did not appear useful in D=2+1.) The first set (third column of masses) differs from the second principally in that on the $L = 14, 16$ lattices we chose less plausible $p = 0$ masses in order to be consistent with the $p = 1$ values with which they were then averaged. In the last 'safe' column we dealt with this discrepancy by not using the $p \neq 0$ values (which, in any case, become much less useful on the smaller lattices). Thus this range of mass estimates gives some indication of any systematic error that arises from our procedure for extracting masses.

We first note that the loop mass increases approximately linearly with the loop length confirming, as expected, that the theory is linearly confining (up to ~ 2.3fm).

In Table 5 we list the values of the effective string correction coefficient, c_s^{eff}, defined in eqn(10). As in D=2+1 our most accurate values of c_s^{eff} are those that incorporate $p \neq 0$ energies, and we display one set of these in Fig.3. We see in the plot a behaviour similar to what we observed in D=2+1: the value of c_s^{eff} increases as the loop length increases, attains a maximum value at $l \simeq 1$fm that is significantly larger than the bosonic string value, and then decreases to a value consistent with the value for a bosonic string.

Just as in D=2+1 we estimate c_s by using eqn(6) to fit all the loop masses that are longer than some reference value l_0. If l_0 is small there is no acceptable fit. As we

increase l_0 we find that the fit eventually becomes acceptable. We then increase l_0 to check the stability of the best fit. In Table 6 we list the results of this procedure for each of our last three sets of loop masses. (For the first set there are no acceptable fits, perhaps indicating that some of the mass choices were indeed too optimistic.) The most accurate values are obtained from the last two sets, and we use these to obtain our best estimate for the string correction:

$$c_s = 0.94 \pm 0.06. \tag{13}$$

This is close to the bosonic string value and far from that of other simple string theories.

5 k-strings

In the previous Section we accumulated some evidence that SU(2) flux tubes in the fundamental representation are described by an effective bosonic string theory at large distances. In this Section we consider flux tubes in higher representations: the k-strings described in the Introduction. We will not be able to perform comparable checks on the stringy nature of these flux tubes although we will perform some crude finite volume analyses that are primarily designed to confirm the presence of linear confinement in SU($N \geq 4$) gauge theories. In our analysis of the string tension ratios, σ_k/σ, we shall make the plausible assumption that the leading correction is that of a simple bosonic string. However for completeness we shall also point out how the results are affected if this should not be the case.

In order to provide some theoretical context within which to view our numerical results, we shall first briefly summarise some of the existing ideas about how such ratios might behave. This is not intended to be an exhaustive review, and our references are merely designed to provide an entry into the literature rather than aiming at completeness.

We then describe our calculations of $k = 2$ and (fundamental) $k = 1$ strings in D=3+1 SU(4) and SU(5) gauge theories. We follow this with a description of our D=2+1 calculations which are for SU(4) and SU(6). In this last case we also have non-trivial $k = 3$ strings that we are able to analyse.

We shall find that in D=3+1 the string tension ratios lie between the predictions of MQCD and Casimir scaling, straddling both within errors; with SU(4) slightly favouring Casimir scaling and SU(5) leaning towards MQCD. In D=2+1 our results are again close to both Casimir scaling and to MQCD, but now they are much more accurate and so we can begin to see significant deviations. Although we see deviations from both sets of predictions, those from MQCD are much larger than those from Casimir scaling. We point out that near-Casimir scaling occurs naturally if the confining flux tube has a cross-section that is independent of the flux carried. We perform calculations in D=2+1 that explicitly demonstrate that this is in fact so. These calculations give us, as a side-product, the value of the k-string tensions at high temperature, and we find

near-Casimir scaling there as well. Motivated by this we perform a high T calculation in the D=3+1 SU(4) gauge theory where we again find near-Casimir scaling.

It is interesting to ask if all this also occurs for the unstable strings. We shall show that our D=2+1 calculations provide some evidence that points to this .

5.1 Some expectations for k-strings

The interest in strings that emanate from sources in higher representations goes back a long way. The early discussions were framed in terms of unstable strings in SU(2) and SU(3) gauge theories as were the lattice calculations. (See, for example, [3].) Despite the uncertainties of this kind of calculation, these early results were already seen as being able to discriminate against particular theoretical ideas; in particular [13] against the bag model [13, 14]. There have been recent much more accurate SU(3) calculations [15, 16] that support this earlier work, and this has sparked some interest in the possible dynamics [17, 18, 19]. The recent interest [20, 5], including our own, in stable k-strings in SU($N \geq 4$) has been largely due to conjectures arising in M(-theory)QCD [2]. Here we briefly allude to some of these theoretical ideas, with a particular focus on MQCD and 'Casimir scaling' since their predictions turn out to be closest to the results we obtain [5, 6] for the tensions of k-strings.

5.1.1 unbound strings

The simplest possibility is that

$$\sigma_k = \tilde{k}\sigma_{k=1} \qquad ; \quad \tilde{k} = \min\{k, N-k\}. \tag{14}$$

That is to say the total flux is carried by k (or $N-k$ if that is smaller) independent fundamental flux tubes. This would occur if the interaction between fundamental flux tubes was so weak that there were no bound or resonant multi-string states. One may regard this as the trivial scenario with which the actual calculated values of σ_k can be contrasted.

5.1.2 Casimir scaling

The idea that the confining flux tube between sources will be proportional to the quadratic Casimir, $C_{\mathcal{R}}$, of the representation of those sources

$$\sigma_{\mathcal{R}} \propto C_{\mathcal{R}} \tag{15}$$

is an old idea. An early motivation [3] arose from a model of 'random fluxes' for the vacuum and the observation that in certain solid state systems this leads to a dimensional reduction $D \to D-2$. Thus $D=4$ theories would reduce to $D=2$ gauge theories in which the Coulomb linear potential is indeed proportional to the quadratic

Casimir. The numerical calculations supporting this were in D=4 SU(2) [3] and thus involved potentials at relatively short distances. The observation soon after that one seemed to see a similar Casimir scaling in D=3 theories [3] forced a generalisation of the dimensional reduction idea [3]. The most accurate early calculations involved the adjoint string tension. Recently however there have been accurate calculations [15, 16] for a variety of representations in SU(3) and this has sparked renewed interest in this idea [17, 18, 19].

There are obvious ambiguities in calculating the string tension of unstable strings from the intermediate distance behaviour of the static potential. At short distances we know that we have a Coulomb potential which, of course, displays Casimir scaling. As the potential interpolates between this and the long-distance behaviour one expects some continuity. If, as is usually done, one fits the potential $V(r)$ by a simple sum of a Coulomb term and a linear piece, $V(r) = V_0 + c/r + \sigma r$, and then performs the fit in a limited range of r immediately beyond the Coulomb region, then it might be that simple continuity artificially forces approximate Casimir scaling on the fitted linear term. While this is no more than a possibility, it does underscore the utility of using stable strings as we shall do, where one can go to larger distances; and doing the calculation in a way, as we shall also do, that does not involve explicit sources and Coulomb terms.

Since the sources may be screened by gluons, which are in the adjoint representation and do not feel centre gauge transformations, it is appropriate, as we remarked earlier, to categorise the representations of SU(N) sources by how they transform under the centre of the group. If the source acquires a factor z^k with $k \in Z_N$, then we shall generically refer to the corresponding flux tube as a k-string. Any k-string can be transformed into any other k-string by appropriate gluon screening. Thus the stable k-string will be the one with the smallest string tension. Any other k-string will, at sufficiently large distances, find it energetically favourable to be transformed into the lightest stable string through gluon screening. If we have Casimir scaling then the lowest string tension corresponds to the representation with the smallest quadratic Casimir, and this is the totally antisymmetric representation. (See the Appendix A.3.) The ratio of these quadratic Casimirs gives us the Casimir scaling prediction for stable k-strings

$$\frac{\sigma_k}{\sigma} = \frac{k(N-k)}{N-1}. \tag{16}$$

5.1.3 MQCD

A number of calculations in brane (M-)theory of QCD-like theories (see [2] and references therein), which are generically referred to as MQCD, find that that the string tension of k-strings satisfies

$$\frac{\sigma_k}{\sigma} = \frac{\sin\frac{k\pi}{N}}{\sin\frac{\pi}{N}}. \tag{17}$$

This led to the conjecture [2] that this might be a universal result and that QCD (and SU(N) gauge theories) fall into this universality class.

This prediction has reasonable properties: it has the required $k \leftrightarrow N-k$ symmetry and takes sensible values for $N = 2, 3$. However the MQCD origins neglect potentially important quantum fluctuations which might [2] renormalise the simple and elegant formula in eqn(17).

The MQCD calculations are, strictly speaking, for SU(N) gauge theories in 3+1 dimensions. It is not clear how much evidence there would be for a corresponding MQCD conjecture in D=2+1, although a naive reading suggests that the brane constructions in [2] would lead to the same conclusion for the σ_k ratios. In any case the trigonometric formula in eqn(17) has the correct qualitative properties and so we shall compare our results to it not only in D=3+1 but also in D=2+1 and, indeed, at finite temperature.

5.1.4 bag model

In the bag model (see e.g. [14, 13]) the flux between distant sources is confined to a cylindrical bag of cross-section A. The flux is homogeneous $E_a A = gT_a$, and the vacuum energy difference between the inside and outside of the bag is given by the bag constant B. Thus the energy per unit length is [14, 13]

$$\frac{E}{l} = 2\pi\alpha_s \frac{C_{\mathcal{R}}}{A} + AB \tag{18}$$

where $C_{\mathcal{R}}$ is the quadratic Casimir of the source and α_s is the strong coupling constant. One now fixes the area A by minimising the energy. This gives the string tension to be

$$\sigma_{\mathcal{R}} \propto \{C_{\mathcal{R}}\}^{\frac{1}{2}} \tag{19}$$

which differs markedly from Casimir scaling. The fact that the early numerical calculations gave an adjoint string tension that satisfied eqn(15) rather than eqn(19) was picked up [13] as providing critical evidence against conventional bag dynamics [14, 13], in that it suggested a flux tube cross-section that was independent of the size of the flux.

5.1.5 strong coupling

In the strong coupling limit, $\beta \to 0$, of our action, a Wilson loop involving k strings will need to be tiled with plaquettes at least k (or $N-k$) times. The leading term in this limit will therefore reproduce eqn(14): $\sigma_k = \tilde{k}\sigma_{k=1}, \tilde{k} = \min\{k, N-k\}$. However the non-leading terms will introduce interactions between these tiled surfaces, and this simple ratio will change as we move away from the strong coupling limit.

Strong coupling predictions are, of course, not universal; however this one is more universal than most. If we generalise the action to contain any combination of closed loops, so long as these are linear in the SU(N) link matrices we will still obtain eqn(14).

However if we include loops or products of loops that are not linear in the links then we can obtain other results. One can think of the action as having loops in different representations, and the value of σ_k/σ will depend only on what these representations are and what are their relative weights. By choosing an action in an appropriate 'universality' class, one can essentially obtain for σ_k/σ any value one wants.

Hamiltonian strong coupling (see e.g. [21]) is more interesting. The leading term, as $g^2 \to \infty$, is simply the quadratic Casimir for each spatial link. Gauss's law means that our two k-sources are joined by excited links, and that the lightest k string will satisfy Casimir scaling as in eqn(16). Of course the magnetic perturbation will spoil this result as we move away from $\beta = 0$.

5.2 k-strings in D=3+1

We will now calculate the ratio of the $k = 2$ and fundamental string tensions, $\sigma_{k=2}/\sigma$, in both SU(4) and SU(5) gauge theories. There are no other stable k-strings for these values of N but having results for two values of N will already provide significant constraints. We are, of course, interested in the continuum limit, so we calculate this ratio for several lattice spacings and then extrapolate to the continuum limit using the fact that for the plaquette action the leading lattice correction to dimensionless mass ratios is $O(a^2)$:

$$\frac{\sigma_k(a)}{\sigma(a)} = \frac{\sigma_k(0)}{\sigma(0)} + ca^2\sigma. \tag{20}$$

We calculate the string tension from the mass of a flux loop that winds around the spatial torus. We assume that the leading correction to the linear dependence of the mass is that appropriate to a simple bosonic string:

$$m_k(l) \stackrel{l\to\infty}{=} \sigma_k l - \frac{\pi(D-2)}{6}\frac{1}{l}. \tag{21}$$

This assumption has some support from the calculations of the previous Section, but it is not guaranteed that what holds for SU(2) holds also for larger N. So we shall occasionally pause to state how sensitive are our results to this assumption.

We begin by listing in Table 7 the (fundamental) string tensions [6] corresponding to the various β values at which we perform our calculations. This sets the scale of a in physical units. In Table 8 we list our lattices and calculated values of the $k = 1$ and $k = 2$ flux loop masses for the case of SU(4); and in Table 9 for SU(5). (Note that in these calculations we only use $p = 0$ correlators.)

In order to extract a string tension from the flux loop mass we must ensure that our loop length is long enough for the corrections to eqn(21) to be negligible within our statistical errors. In Section 4.2 we have seen that in the case of SU(2) this appears to be the case for strings longer than $l\sqrt{\sigma} \equiv La\sqrt{\sigma} \simeq 3$ (see Tables 5,6). Here we perform an additional finite size study, this time in SU(4), which, while less accurate, will probe the behaviour of $k = 2$ as well as $k = 1$ strings.

Our finite size study is at $\beta = 10.7$ and involves loops ranging from $L = 6$ to $L = 16$ with masses as listed in Table 8. The longest length translates into $l \simeq 4.9/\sqrt{\sigma} \simeq 2.2$fm. We observe that both the $k = 2$ and $k = 1$ masses grow approximately linearly with l, demonstrating that the SU(4) theory linearly confines both $k = 1$ and $k = 2$ charges (at least over this distance range). Using eqn(21) we extract the ratio $\sigma_{k=2}/\sigma$ which we plot in Fig.4. We see that within errors the ratio becomes independent of the flux loop length for $l \geq 10a \simeq 3/\sqrt{\sigma}$. For comparison we also show what happens if we do not include any string correction at all, i.e. $\sigma_{k=2}/\sigma = m_{k=2}(l)/m_{k=1}(l)$. We see that while the ratio changes by a few percent, it becomes independent of l, within errors, at the same length, $l = 10a$. By the same token it is clear that the results of this calculation are not accurate enough to distinguish between different possible string corrections.

Our finite volume study has taught us that higher order corrections in $1/l$ to the string tension ratio will be negligible (within our typical errors) if we make sure that our loop length satisfies $l\sqrt{\sigma} \geq 3$. Comparing the values of $a\sqrt{\sigma}$ in Table 7 with the corresponding lattice sizes listed in Table 8 and Table 9 we see that our loop lengths have been chosen to fulfill this bound; more generously at smaller a where the errors are smaller.

Assuming eqn(21), we extract our string tension ratios and plot them against $a^2\sigma$ in Fig. 5. (At $\beta = 10.7$ we use only the $L = 10, 12$ lattices since the larger volumes have errors that are too large to be useful.) On such a plot the continuum extrapolation, eqn(20), is a simple straight line. We show the best such fits in Fig. 5. We find that if we use all the points we get an excellent χ^2 for SU(4) and an acceptable one for SU(5). From these fits we obtain the following continuum values:

$$\lim_{a\to 0} \frac{\sigma_{k=2}}{\sigma} = \begin{cases} 1.357 \pm 0.054 & \text{SU(4)} \\ 1.58 \pm 0.10 & \text{SU(5)} \end{cases} . \tag{22}$$

One might worry that these fits could be biased by including the coarsest a value (where we know [6] the lattice corrections to the scalar glueball mass to be large). If we exclude this coarsest a point our best values in eqn(22) are changed to:

$$\lim_{a\to 0} \frac{\sigma_{k=2}}{\sigma} = \begin{cases} 1.377 \pm 0.063 & \beta \geq 10.70 & \text{SU(4)} \\ 1.76 \pm 0.16 & \beta \geq 16.975 & \text{SU(5)} \end{cases} . \tag{23}$$

This gives us some idea of the direction of any such bias.

It is interesting to compare our results with the expectations of MQCD

$$\frac{\sigma_{k=2}}{\sigma} \stackrel{MQCD}{=} \frac{\sin\frac{2\pi}{N}}{\sin\frac{\pi}{N}} = \begin{cases} 1.41... & \text{SU(4)} \\ 1.61... & \text{SU(5)} \end{cases} \tag{24}$$

and Casimir scaling

$$\frac{\sigma_{k=2}}{\sigma} \stackrel{CS}{=} \frac{k(N-k)}{N-1} = \begin{cases} 1.3\bar{3} & \text{SU(4)} \\ 1.50 & \text{SU(5)} \end{cases} . \tag{25}$$

We see that our results in eqn(22) (and eqn(23)) are consistent with both these expectations, within quite small errors; with perhaps a slight bias towards favouring MQCD. It is because the two sets of predictions are numerically very similar that we cannot, at present, choose between them. On the other hand we clearly exclude the unbound string value of 2: i.e if we do wish to think of the $k = 2$ string as being composed of two $k = 1$ strings then it must be a tightly bound state of such strings. We also clearly exclude the bag model prediction:

$$\frac{\sigma_{k=2}}{\sigma} \stackrel{Bag}{=} \sqrt{\frac{k(N-k)}{N-1}} = \begin{cases} 1.15... & \mathrm{SU}(4) \\ 1.22... & \mathrm{SU}(5) \end{cases} . \tag{26}$$

In order to distinguish clearly between MQCD and Casimir scaling we need to reduce our statistical errors by about a factor of two; a feasible goal but one for the future.

Thus our conclusions are essentially unchanged from those of our earlier paper [5] although our SU(4) calculation now has smaller statistical errors, and our SU(5) calculation is now free of the potentially large systematic errors that concerned us earlier.

A final remark. Our above analysis assumed that the flux tubes behave like simple bosonic strings. What difference does it make if we do not make this assumption? Suppose first that we use the result we obtained in Section 4.2 for the coefficient of the string correction: $c_s = (1.25 \pm 0.25)\pi/3$ (where we take very generous errors). Repeating our analysis with such a string correction we find that our results in eqn(22) are lowered by about 10% of the statistical error; that is to say, insignificantly. Even if we were to ignore what we knew and simply assumed some range like $c_s = (1 \pm 1)\pi/3$ we would find that the maximum shift would be less than our quoted statistical error. (For $c_s = 0$ the ratios are close to MQCD while for $c_s = 2\pi/3$ they drop very close to Casimir scaling.)

5.3 k-strings in D=2+1

Our calculations in D=2+1 follow the same pattern as in D=3+1 except that our calculations are in SU(4) and SU(6). The main reason for SU(6) rather than SU(5) is that with the former one also has stable k=3 strings that one can study. On the other hand the calculations take longer which is why we contented ourselves with SU(5) in four dimensions. Our calculations are summarised in Tables 11 and 12 and the scale of a, in units of the fundamental string tension, is given in Table 10.

We begin with a finite volume study in SU(4) at $\beta = 28.0$ that parallels our D=3+1 study. The loop lengths range from $L = 4$ to $L = 16$, with the largest loop corresponding to $l = 16a \simeq 4/\sqrt{\sigma} \simeq 1.6$fm. We extract $\sigma_{k=2}/\sigma$ using eqn(21) and plot the result in Fig.6. We see that the ratio of string tensions is independent of the loop length (within errors) once $l \geq 10a \simeq 2.5/\sqrt{\sigma} \simeq 1.1$fm. This is a somewhat shorter length than the one we found in D=3+1. We shall later see that the flux tube is thinner (in units of σ) in D=2+1 than in D=3+1 and this is presumably why the corrections are

smaller. We also show in Fig.6 the string tension ratios one obtains if one assumes no correction. This also plateaus for $l \geq 10a$. Moreover we see that the value of the ratio differs by only about 1%. (Note the string correction is $\propto (D-2)$ and so is larger in D=3+1 than in D=2+1.)

We observe that the loop lengths we shall use, as listed in Tables 11 and 12, satisfy the above bound, $l \geq 2.5/\sqrt{\sigma}$, by a good margin. So assuming eqn(21), we plot our string tension ratios in Fig. 7 against $a^2\sigma$. We also show the straight line continuum extrapolations, using eqn(20). We find that we get an acceptable χ^2 using all the points. We thus obtain the following continuum values:

$$\lim_{a\to 0} \frac{\sigma_{k=2}}{\sigma} = \begin{cases} 1.355 \pm 0.010 & \text{SU(4)} \\ 1.616 \pm 0.013 & \text{SU(6)} \end{cases} \tag{27}$$

and

$$\lim_{a\to 0} \frac{\sigma_{k=3}}{\sigma} = 1.808 \pm 0.040 \quad \text{SU(6)}.. \tag{28}$$

We note that the errors here are much smaller than in eqn(22) and the MQCD expectation is excluded. We also see, in our $k = 2$ SU(4) ratio, a deviation from Casimir scaling at the level of 2 to 2.5 standard deviations. In SU(6) the expectations are

$$\frac{\sigma_{k=2}}{\sigma} \overset{SU(6)}{=} \begin{cases} 1.73... & \text{MQCD} \\ 1.60 & \text{CS} \end{cases} \tag{29}$$

and

$$\frac{\sigma_{k=3}}{\sigma} \overset{SU(6)}{=} \begin{cases} 2.0 & \text{MQCD} \\ 1.8 & \text{CS} \end{cases} . \tag{30}$$

We see that our results are far from the MQCD values and agree well with Casimir scaling.

Given our very small statistical errors one might worry that our assumption of a bosonic string correction might introduce a relatively large systematic error. In fact this is not so. If we take our SU(2) string analysis in Section 4.1 to be telling us that the coefficient of the $1/l$ term is $c_s = (1.1 \pm 0.1)\pi/6$, then we find a negligible shift in our above predictions. Even if we were to assume $c_s = 0$ this would shift our values upwards by less than 2%. While this would increase the deviation from Casimir scaling, generally it would be far from enough to bridge the gap to the MQCD prediction. However $c_s = 0$ is a contrived and extreme example, and it appears to us that any reasonable estimate of the systematic error arising from the uncertainty in the string correction shows it to be negligible.

5.4 Width of k-strings

We have seen that in both D=2+1 and D=3+1 the ratio σ_k/σ is close to the Casimir scaling value. In D=3+1 it is also consistent with MQCD, but the MQCD and Casimir

scaling predictions are in fact quite close. If one imagines modelling the flux tube then this is a somewhat conter-intuitive result. It would be natural to think of the flux as homogeneous and that the vacua inside and outside the flux tube differ by some energy density δE_v. These are of course the ideas embodied in the Bag model. One would then expect that as the representation of the flux increases, so that the chromoelectric energy density increases, the area will increase so as to minimise the total energy increase. This is just the variational calculation of the naive bag model which leads to a ratio σ_k/σ that grows as the square root of the quadratic Casimir. This is definitely excluded by our calculated values. One might imagine extending this simple-minded model by providing the flux tube with a surface tension. However this would have no effect in D=2+1 where the surface is independent of the flux tube width.

If the flux is homogeneous and if the flux tube width is independent of the total flux carried, then one naturally obtains Casimir scaling. If one considers a superconductor, in a phase that exhibits the Meissner effect and supports (magnetic) flux carrying flux tubes, there is a range of parameter values, called the deep-London limit, where the flux tube cross-section is indeed independent of the flux (see e.g. [22]). This corresponds to a penetration depth, related to the photon mass, being much larger than the inverse scalar Higgs mass. The deviation from Casimir scaling would be related to the ratio of these masses.

It is interesting to test these ideas. Here we shall attempt to calculate the widths of the flux tubes corresponding to different k-strings and see how close the width is to being independent of k. We shall do so in D=2+1 because it is faster; but the same technique can be used in D=3+1. We shall perform calculations for $k = 1, 2$ flux tubes in SU(4) and for $k = 1, 2, 3$ flux tubes in SU(6).

We use a technique that was employed in [23] to calculate the width of SU(2) flux tubes in D=2+1. Consider a lattice of size $L \times L_\perp \times L_t$. L_t refers to the Euclidean time in which we calculate correlations. The flux loop is of length L, and $L_\perp$ is the spatial size transverse to the flux tube. By reducing $L_\perp$ we can squeeze the flux tube. If the flux tube oscillates with simple harmonic modes then it will not be affected by reducing the finite (periodic) transverse width until it reaches the 'intrinsic' width of the flux tube [23]. Once $L_\perp$ is smaller than this width, which we shall call $l_w = aL_w$, we expect the mass of the flux loop to increase as [23]

$$am(L; L_\perp) = am(L; \infty) \times \frac{L_w}{L_\perp} \ . \tag{31}$$

The onset of the increase is at $L_\perp = L_w$ and provides us with an estimate of L_w. Our main interest is to see if L_w varies with k or not.

Of course the above arguments are very simple. There are changes in the vacuum as $L_\perp$ becomes small. Indeed there is a phase transition at a critical value of $L_\perp$ (see Section 5.5) which is characterised by the development of a non-zero vacuum expectation value for the Polyakov loops that wind around the short $L_\perp$ torus. However the string tensions we calculate behave smoothly through this transition, suggesting

our simple analysis should not be invalidated. In any case, our main conclusion, that as k grows the flux tube width does not grow ever larger, will remain valid since such a growth would mean that higher k flux tubes would begin to be squeezed when $L_\perp$ was greater than its critical value, and this would certainly be visible.

We show in Table 13 how $am_k(L;L_\perp)$ varies with $L_\perp$ for $k=1$ and $k=2$ flux tubes; all at $\beta=28$ in the SU(4) gauge theory in D=2+1. We do so for $L_\perp=2,...,20$ and for two values of the flux tube length, L. The minimum transverse size is $l_\perp = aL_\perp = 2a \simeq 0.5/\sqrt{\sigma}$ which we expect to be smaller than l_w. The loop lengths are $l=aL=8a,12a \simeq 0.9,1.35$fm which should be long enough to allow well-formed flux tubes. We calculate masses for two values of L at each $L_\perp$ in order to check whether the mass is growing nearly linearly with L and that we do indeed have a flux tube. We see from the masses listed in Table 13 that this is so for all values of $L_\perp$.

We plot the $L=8$ flux loop masses in Fig.8. We see that both $m_{k=1}$ and $m_{k=2}$ start increasing at a very similar value of $L_\perp$. Moreover the masses for the smallest two values of $L_\perp$ are consistent with eqn(31). If we take these to fix the value of L_w in eqn(31), we find that $L_w \simeq 5.2$ for both $k=1$ and $k=2$ flux tubes. That is to say, the flux tube width is indeed independent of the flux, and has a value $l_w \simeq 1.3/\sqrt{\sigma}$.

In addition to these gross features we also see in Table 13 and Fig.8 that there is a decrease in the mass at values of $L_\perp$ that are just above the values where the mass starts to increase. Moreover this decrease is more pronounced for the $k=2$ string than for the $k=1$ string. Such an effect indicates that there are some difference between the sizes of the two flux tubes – if only in their tails – and an analysis of this might provide information on the dynamics, e.g. the parameters of the effective dual superconductor referred to earlier. However anything quantitative needs calculations with more resolution, i.e at smaller values of a.

We display in Fig.9 how $\sigma_{k=2}/\sigma$ varies with $L_\perp$. We see that the ratio is close to Casimir scaling not only at large $L_\perp$ (something we have seen already) but also at small $L_\perp$. There is only a small range of $L_\perp$, coinciding with the dip in m_k, where the ratio drops below this. Of course, at very small values of $L_\perp$ our D=2+1 system is effectively reduced to D=1+1 where the linear confinement of the gauge theory arises through the Coulomb interaction and this automatically satisfies Casimir scaling.

Our SU(6) analysis closely parallels our SU(4) analysis except for the fact that we now have additional $k=3$ strings. Our calculations are at $\beta=60$ which, as we see from Table 10, has a similar a to that at $\beta=28$ in SU(4).

Our masses are listed in Table 14. They are for flux loops of length $l=10a$ and $l=12a$ and once again we see evidence for a linearly growing mass for all k and for all $L_\perp$. We plot the $L=10$ flux loop masses in Fig.10 and we see, once again, an increasing loop mass at small $L_\perp$ that is consistent with eqn(31). Indeed we find a common flux tube width, $L_w \simeq 4.5$, for all three values of k. So, just as in SU(4), the flux tube width is independent of the flux, and has a value $l_w \simeq 4.5a \simeq 1.2/\sqrt{\sigma}$ that is also very similar. Again, just as in SU(4), the loop mass decreases just before it begins

to increase.

We plot σ_k/σ in Fig.11. We again see consistency with Casimir scaling at small as well as at large $L_\perp$, except possibly in the region of the dip.

This analysis thus appears to confirm that the confining flux tube has a cross-section that is largely independent of the flux carried. The minor differences between k-strings might, however, be useful in telling us about the details of the confinement mechanism.

5.5 High T spatial string tensions

In our above calculations we have calculated the mass of a long flux loop in a spatial volume with a limited transverse spatial dimension, $L_\perp$. Let us relabel the axes of our $L \times L_\perp \times L_t$ lattice so that the short spatial torus becomes our time torus and our time torus becomes a long spatial torus. We are now on a $L_x \times L_y \times L_t$ lattice with $L_t = L_\perp$ and $L_x, L_y \gg L_t$. This corresponds to a system at temperature $aT = 1/L_\perp$. and, as we decrease $L_\perp$, we will pass through the deconfining phase transition at $T = T_c$. In this rotated co-ordinate system the flux loop 'mass' that we have calculated is obtained from the spatial correlation of spatial loops; it is a screening mass, from which we can calculate what is usually referred to as the 'spatial string tension' (usually obtained from spatial Wilson loops). Thus our finite width studies have in fact provided us with a calculation of the $k = 1$, $k = 2$ and $k = 3$ spatial string tensions as a function of T in SU(4) and SU(6) D=2+1 gauge theories. (All this parallels previous studies [23, 24] of SU(2) in D=2+1.)

Simple arguments (see for example [24]) tell us to expect $\sigma \propto g^2 T$ for $T \gg T_c$. In our case, where $aT = 1/L_t = 1/L_\perp$, this translates to $a^2\sigma \propto 1/L_\perp$ as $L_\perp \to 0$. This is precisely what we have already inferred from the SU(4) and SU(6) calculations in Tables 13 and 14. Indeed we see that the linear increase with T sets in very close to $T = T_c$, and does so simultaneously for all k-strings. (Although we do not have precise calculations of the deconfining temperatures in SU(4) and SU(6) gauge theories, we expect from extrapolations of previous SU(2) and SU(3) calculations that $T_c \simeq 0.95\sqrt{\sigma}$ in D=2+1 and this tells us that the critical value of $L_\perp$ is ~ 4 at these values of β.) Moreover, as we see from Figs. 9 and 11, the string tension ratio is close to the value expected from Casimir scaling. This is not a great surprise: the high-T dimensional reduction of the D=2+1 theory takes us to a D=1+1 theory, and in a D=1+1 gauge theory even the Coulomb potential is linearly confining; and the latter will automatically satisfy Casimir scaling. This is of course simplistic; the dimensional reduction leads to (adjoint) scalars as well as gauge fields, in the reduced theory and, in any case, the linear potential may have other sources than just the Coulomb potential.

We now turn to the more interesting case of D=3+1. We shall not attempt a systematic study but, just as in D=2+1, we shall work at one single value of β and will vary T in the rather coarse steps allowed by varying L_t. Our calculation is in SU(4) at $\beta = 10.7$. Although we do not have precise information on the deconfining temperature, an extrapolation of previous SU(2) and SU(3) calculations [25] using a

simple $O(1/N^2)$ correction, suggests that $T_c \simeq 0.62\sqrt{\sigma}$ for SU(4). Since $a\sqrt{\sigma} \simeq 0.306$ at $\beta = 10.7$ (see Table 7) the critical value of L_t is ~ 5. Thus a spatial volume of 10^3 should be adequately large for our exploratory calculation. Accordingly we work on the $10^3 L_t$ lattices listed in Table 15. In the Table we also include our earlier calculations on a 10^4 lattice, to provide the '$T = 0'$ reference value.

We first wish to establish the rough location of T_c. To do so we calculate $\langle l_p \rangle$, the average of the thermal line (an unblocked Polyakov loop that winds once around the Euclidean time-torus), the lightest mass, am_t, that contributes to spatially separated correlations of such lines, and $\langle Q^2 \rangle$, the average value of the fluctuations of the topological charge Q. It is clear that, as expected, there is a phase transition close to $L_t = 5$: the thermal line develops a non-zero vacuum expectation value, and consequently the lightest mass becomes ~ 0 (the energy of the vacuum). We also see a very striking suppression of the topological susceptibility, $a^4\chi_t \equiv \langle Q^2 \rangle / (L^3 L_t)$ across $L_t = 5$. One observes a similar but much less dramatic behaviour in SU(3) [26], and this suggests that χ_t might be an order parameter for the deconfining phase transition, at least as $N \to \infty$, with appropriate consequences for the axial U(1) anomaly. This is a topic we shall expand upon elsewhere.

Having established what is 'high' T in our calculation, we show in Table 16 the (screening) masses one obtains from spatially separated correlators of $k = 1$ and $k = 2$ loops that wind once around the spatial torus. At high T we expect $\sigma \propto T^2$ (since g^2 is now dimensionless). We see that while our flux loop masses grow faster than T they grow less fast than T^2. This should be no surprise; rather one should be surprised by the precociously early onset of the linear high-T behaviour in the case of D=2+1.

From the flux loop masses we calculate the string tension in two ways: assuming no string correction, i.e. setting $c_s = 0$ in eqn(6), and assuming a bosonic string correction. One might expect that at high T one should use a string correction that is half-way between, because one has lost one of the transverse dimensions. In any case it is clear that the high-T ratio is consistent with Casimir scaling but probably not with the MQCD formula. Just as for D=2+1 we see a dip in the masses at T just below T_c. By contrast, for this lattice calculation, the low-T calculation on the 10^4 lattice is consistent with MQCD but not really with Casimir scaling.

Once again one might try to use dimensional reduction to relate the Casimir scaling we observe at high T in D=3+1 to our observation of it, earlier on in this paper, at low T in D=2+1. However any such argument must address the caveats created by the presence of extra adjoint scalars after the reduction. We also note that Casimir scaling – at least for k-strings and at very high T – has been predicted in a recent model calculation [27] which speculates that at high T there is a plasma of adjoint magnetic pseudoparticles 'dual' to the gluon plasma. (Again one might try to relate [27] this to low-T near-Casimir scaling in D=2+1 via dimensional reduction.)

5.6 Unstable strings

Our calculations have so far focussed on stable k-strings. In addition to these, there are also unstable strings, which are energetically unfavourable. Unstable strings should appear as a nearly stable excited state in the k-string spectrum. It is clearly interesting to find out how the string tensions of these strings depend on their representation and on N. We note that this is precisely the question addressed by the calculations in, for example, [3, 15, 16]. In this Section we will investigate closed strings with the quantum numbers of strings connecting k quarks in a given irreducible representation for $k = 2, 3$.

The tensions of strings connecting sources in a given irreducible representation can be extracted from correlation functions of operators carrying the quantum numbers of that representation. For $k = 2$ the irreducible representations with two quarks are the symmetric and the antisymmetric representations. At $k = 3$ the irreducible representations with three quarks are the totally antisymmetric, the totally symmetric and the mixed symmetry representation, which enters twice the decomposition of the tensor product. The general procedure to construct the relevant operators for a given representation and the explicit form of the operators corresponding to the cases we shall investigate in this Section are given in Appendix A.1.

At each $\mathcal{N}$-lity (and at finite N) only the string with the smallest tension is stable. For any k, this string is expected to be the string connecting k sources in the totally antisymmetric representation. Hence the smallest mass in the antisymmetric channel is related to the string tension at the given $\mathcal{N}$-lity. Our calculations fulfill this expectation: the smallest mass extracted with the variational procedure and the smallest mass in the antisymmetric channel always agree well within errors, both in D=2+1 and D=3+1.

At fixed length an unstable k-string is more massive than the stable string of the same $\mathcal{N}$-lity. This is likely to give problems when looking at the exponential decay in time of correlation functions: the signal will decay too rapidly to allow a reliable extraction of masses. Indeed this is what happens in our D=3+1 calculations: given the precision of our numerical data, it proves to be impossible to extract reliable masses. To overcome this problem, we should get closer to the continuum limit or use anisotropic lattices. We leave such a study for the future. Another crucial point is the overlap between the operators and the interesting states, which if the operators are constructed using standard techniques (as we have done in the present study) can get as bad as 0.5 for unstable strings in D=3+1. (For comparison, always in D=3+1 the overlap between the stringy state corresponding to the antisymmetric representation and our operators is at worse around 0.8-0.85.) Hence, to address questions connected to unstable strings a better overlap is required. This requires in turn an improvement of the standard smearing techniques. This is another problem we will investigate in the future.

While we can not deal at the moment with unstable strings in D=3+1, our numerical results in D=2+1 allow us to address the question there. In fact, our D=2+1 calculations do not suffer from the same drawbacks as the D=3+1 ones: our D=2+1

results are accurate enough to see a clear exponential decay of the correlation functions over several lattice spacings and in D=2+1 the overlap between the operators and the unstable strings is not worse than 0.85. Our numerical results for SU(4) and SU(6) are reported respectively in Tables 17 and 18. Apart from the symmetric representation of SU(6), for which we have masses for just two values of the lattice spacing, we can extrapolate the string tensions extracted from the masses listed in the Tables to the continuum limit by applying the same procedure used for stable strings. We then find

$$\lim_{a\to 0}\frac{\sigma_{k=2S}}{\sigma}=\begin{cases}2.14\pm 0.08 & \mathrm{SU}(4)\\ 2.19\pm 0.04 & \mathrm{SU}(6)\end{cases} \tag{32}$$

for the string tensions in the $k=2$ symmetric channels and

$$\lim_{a\to 0}\frac{\sigma_{k=3M}}{\sigma}=2.71\pm 0.17 \quad \mathrm{SU}(6) \tag{33}$$

for the $k=3$ mixed symmetry channel. (The string tensions have been extracted using the bosonic string correction.) For the continuum value of the $k=3S$ string tension, an estimate based on our data gives

$$\lim_{a\to 0}\frac{\sigma_{k=3S}}{\sigma}\approx 3.7 \quad \mathrm{SU}(6). \tag{34}$$

Our numerical results can be compared with the predictions coming from Casimir scaling

$$\frac{\sigma_{k=2S}}{\sigma}=\begin{cases}2.40 & \mathrm{SU}(4)\\ 2.28... & \mathrm{SU}(6)\end{cases}, \tag{35}$$

$$\frac{\sigma_{k=3M}}{\sigma}=2.82... \quad \mathrm{SU}(6), \tag{36}$$

$$\frac{\sigma_{k=3S}}{\sigma}=3.85... \quad \mathrm{SU}(6). \tag{37}$$

As for the stable k-strings, these ratios suggest approximate Casimir scaling. As far as comparison with MQCD is concerned, we are not aware of calculations in that framework aimed to determine the string tensions of unstable strings.

6 Discussion

Our calculations in this paper were in two parts. In the first part we investigated directly the stringy nature of long flux tubes by calculating how the mass of a flux tube varies with its length l, and attempting to identify the $O(1/l)$ term that is the leading string correction at large l. The coefficient of this term, c_L, is directly related to the central charge of the effective string theory describing the long-distance physics of the confining flux tube, and thus characterises its universality class. By considering

flux tubes that wind around a spatial torus we are able to avoid the presence of explicit sources and the accompanying Coulomb term which can so easily be confused with the string correction. Working in SU(2) and at a reasonably small value of the lattice spacing a, we obtained in 3+1 dimensions a value $c_L = 0.98 \pm 0.06$ which is consistent with the simple bosonic string, for which $c_L = \pi/3$. In 2+1 dimensions we obtained $c_L = 0.560 \pm 0.024$, which is again consistent with the bosonic string value, which is $c_L = \pi/6$ in this case. In both dimensions our results would appear to exclude other plausible possibilities with, for example, some massless fermionic modes along the string. In addition, in the case of D=2+1 our results were accurate enough to constrain the power of $1/l$ to be unity (assuming it to be an integer) as one expects for an effective string theory. These results considerably increase, we believe, the evidence for the simple bosonic string model. There is however much scope for improving these calculations; not only in their accuracy and in the range of flux tube lengths studied, but also in exploring other values of a, so as to be confident of the continuum physics, and in extending the calculations to other SU(N) groups.

The second part of the paper dealt with k-strings in SU($N \geq 4$) gauge theories and, in particular, with the ratios of their string tensions, σ_k/σ. Here we performed a range of calculations so as to be able to extrapolate to the continuum limit. In our D=3+1 SU(4) and SU(5) calculations we found that the $k = 2$ string tension is much less than twice the fundamental $k = 1$ tension: the k-string is 'strongly bound'. Moreover the values are consistent with the M(-theory)QCD conjecture and with Casimir scaling. (These are numerically quite similar.) In our SU(4) and SU(6) calculations in D=2+1 we also found strongly bound k-strings. However, although the calculated string tension ratios were again numerically close to both Casimir scaling and the MQCD formula, the results were accurate enough for us to see that the former works much better, and to observe deviations from both formulae. In addition to these continuum calculations we performed some finite temperature calculations at fixed a which showed that at high T, above the deconfinement transition, 'spatial' k-string tensions are consistent with Casimir scaling, in both 2+1 and 3+1 dimensions. Moreover we found fairly convincing evidence, in D=2+1, for the approximate Casimir scaling of unstable strings. While it might be elegant if (approximate) Casimir scaling were to hold in D=3+1 as well as in D=2+1, and at high T as well as at low T, the fact is that 3+1 dimensions may well differ from 2+1 dimensions, and it is important to perform calculations that are accurate enough to resolve between MQCD and Casimir scaling in D=3+1. Essentially this would require reducing our errors by a factor of two or three; an entirely feasible goal.

We observed that near-Casimir scaling will naturally arise if the chromo-electric flux is homogeneous and the cross-section of the flux tube is (nearly) independent of the flux carried. We pointed out that the latter is not as implausible as it might at first seem: indeed it is what occurs in the deep-London limit of a superconductor. To address this possibility we performed some explicit numerical calculations of the k-string

width and these indicated that the width is indeed largely independent of k. The small k dependence that we did observe can, in principle, be related to the parameters of the dual superconductor, if such is the dynamics of confinement, and we intend to address this question elsewhere. There are a number of other interesting theoretical questions that this work suggests. How closely is the observed near-Casimir scaling of the ('spatial') k-strings at high-T in D=3+1 and at low T in D=2+1 related by dimensional reduction? Equally, is the near-Casimir scaling at high-T in D=2+1, a simple reflection of the Casimir scaling of the linearly confining Coulomb interaction in D=1+1? This requires understanding whether the adjoint scalars, present after dimensional reduction, significantly affect the string tension ratios. Another interesting question is how the string tension ratios, whether given by MQCD or Casimir scaling, reflect themselves in k-vortex condensates, in the dual disorder loop approach to confinement [28], and whether this exposes any simple duality between Wilson loops and 't Hooft disorder loops. A calculation, illustrating how one might proceed, was outlined in [5, 24]. A similar question can be posed in monopole models of confinement, following upon the simple model calculations of higher charged string tensions in [29], after Abelian projection, and in [27] with adjoint monopoles (at high T). A quite different question is what are the implications of these tightly-bound k-strings for the mass spectrum of SU(N) gauge theories. A simple and attractive model sees the glueball spectrum as arising from excitations of closed loops of fundamental flux [30]. In such a model a non-trivial k-string would provide a new sector of states whose masses are scaled up by a simple factor of σ_k/σ [31]. The observation of something like this, when comparing the SU(3) and SU(4) spectra for example, would provide striking information on glueball structure. While our D=3+1 mass spectrum calculations [6] are too crude to usefully explore this question, this is not the case in D=2+1 (see e.g. [1]) and work on this question is proceeding.

Note added: As this paper was being completed, a paper appeared [32] containing a calculation of $k = 1, 2, 3$ string tensions in D=3+1 SU(6). The continuum string tension ratios in [32] agree with the MQCD formula and, as stressed in [32], show a deviation from Casimir scaling that is large compared to the errors. We note, however, that if instead of using the procedure in [32] one extracts the continuum ratios from their lattice ratios using a $O(a^2)$ correction, as we have done in our calculations in this paper, then the errors are larger and the deviation from Casimir scaling is no longer very significant. Thus, given a comparable analysis, the results of [32] are consistent with and complement ours.

Acknowledgments

We are grateful to Gunnar Bali, Luigi Del Debbio, Ian Kogan, Ken Konishi, Chris Korthals Altes, Alex Kovner, Simone Lelli, Paolo Rossi, Riccardo Sturani, Bayram Tekin, Alessandro Tomasiello, Ettore Vicari and numerous other colleagues, for useful communications and discussions. Our calculations were carried out on Alpha Compaq workstations in Oxford Theoretical Physics, funded by PPARC and EPSRC grants. One of us (BL) thanks PPARC for a postdoctoral fellowship.

Appendix

This Appendix collects detailled proofs of some statements contained in the main exposition. In Section A.1 we will derive the explicit form of the operators carrying the quantum numbers of k-strings. In Section A.2 we will show how sources in a given representation can be screened by gluons. Finally, Section A.3 will deal with the quadratic Casimirs of irreducible representations of SU(N) and their relationship with Casimir scaling. Our calculations will be heavily based on Group Theory. In order to make this Appendix self-contained, we will recall some general results of Group Theory. For a wider introduction to the group theoretical background we refer to [33].

A.1 Irreducible representations of SU(N) and k-stings

SU(N) is the group of $N \times N$ unitary matrices. By definition, an object q^i ($i = 1, \ldots, N$) transforms under the fundamental representation of SU(N) if under the action of the group

$$q^i \overset{SU(N)}{\to} U^i_j q^j, \tag{38}$$

$U \in$ SU(N) being the matrix that implements the transformation.

The conjugated representation is related to the fundamental one by complex conjugation. Following the standard notation, we indicate by q_i an object transforming under the conjugated representation. For $N \geq 3$ the fundamental and the conjugated representations are independent. In the following, we will call *quarks* objects transforming under the fundamental representation and *antiquarks* objects transforming under the conjugated representation of SU(N). This terminology reflects the physics of QCD.

Objects transforming under higher representations can be constructed from the tensor product of quarks and antiquarks, and their transformation laws can be easily deduced from the transformation law of the fundamental constituents. For instance

$(q \otimes q)^{ij} = q^i q^j$ under the action of SU(N) transforms as follows:

$$q^i q^j \overset{SU(N)}{\rightarrow} U^i_k U^j_l q^k q^l. \tag{39}$$

The $\mathcal{N}$-lity of a representation is defined as the number of quarks minus the number of antiquarks modulo N. $\mathcal{N}$-lities $k \leq N/2$ and $N-k$ are related by complex conjugation. Since that operation corresponds to charge conjugation, these two $\mathcal{N}$-lities are physically undistinguishable in SU(N) gauge theories.

The concept of $\mathcal{N}$-lity at zero temperature is related to the symmetry under the centre of the gauge group, Z_N: under such symmetry an object of $\mathcal{N}$-lity k pick up a phase $e^{(2\pi i k n)/N}$, $n = 0, 1, \ldots, N-1$. Since the centre symmetry at zero temperature is a good symmetry of the gauge theory and the gluons carry zero $\mathcal{N}$-lity, states with different $\mathcal{N}$-lity cannot mix.

In this paper, we are interested in the tensions of strings connecting sources with $\mathcal{N}$-lity $k \geq 1$. Because of charge conjugation, the string tension associated to states of $\mathcal{N}$-lity $k \leq N/2$ and $N-k$ is the same. Hence we restrict ourself to $k \leq N/2$, that is to say to states constructed from the tensor product of k quarks. (We will briefly discuss states with more than N quarks and why there are supposed to be irrelevant at large N in the two following Sections.) At a given N the independent number of stable k-strings is given by the integer part of $N/2$.

As for the fundamental string, the string tension of a k-string can be extracted by looking at the exponential decay of correlators of loop operators with the quantum numbers of that string. In order to identify the relevant operators, it is useful to decompose the tensor product of k quarks into irreducible representations[1]. To this purpose, the Young tableau technique can be used.

A Young diagram is a two-dimensional ensemble of boxes joined by one edge that respects the following rules:

1. counting the rows from the top to the bottom, the number of boxes in the row i is greater than or equal to the number of boxes in the row j if $i < j$;

2. counting the columns from the left to the right, the number of boxes in the column i is greater than or equal to the number of boxes in the column j if $i < j$.

A valid Young tableau is for instance the following:

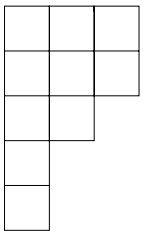

[1]In the following, even if we will omit for simplicity the word *irreducible* from time to time, we will consider only irreducible representations of the gauge group.

In the Young tableau language, a quark is a single box, an antiquark is a column of $N-1$ boxes and an object transforming under the adjoint representation (*gluon*) has $N-1$ boxes in the first column and 2 boxes in the first row:

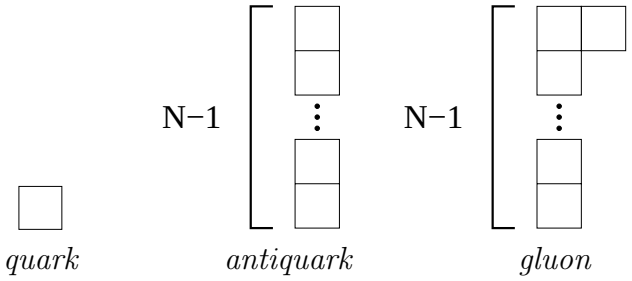

There is a one-to-one correspondence between Young diagrams and irreducible representation of SU(N). Given a Young diagram, the object transforming under the corresponding irreducible representation is constructed from the tensor product of quarks by assigning an index to each box, symmetrising the product with respect to the indices that are on a given row for all rows and then antisymmetrising the result with respect to the indices that are on a given column for all columns. (Obviously, after the antisymmetrisation the result is no longer symmetric under permutation of indices on the same row.)

The tensor product of two objects transforming under two given representations of the gauge group is constructed from the corresponding Young diagrams according to the following rules:

1. write down the two tableaux A and B say labelling each box in the row i of B by i;

2. add the boxes of B to A one-by-one in all the possible positions respecting the following rules:

   (a) the diagram obtained by A at each stage must be a legal Young diagram;

   (b) boxes with the same label must not appear in the same column;

   (c) If we define at any given box position n_j numbers (j being the number of rows in B), each of them counting how many times the corresponding label of the boxes in B appears above and to the right of such a box, we must have $n_1 \geq n_2 \geq \ldots \geq n_j$;

3. two diagrams with the same shape and the same labels are the same diagram;

4. columns with N boxes must be canceled, since they correspond to the trivial representation of SU(N).

According to the above rules, the tensor product of two quarks decomposes as

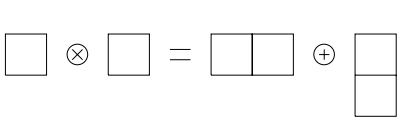

i.e. the irreducible representations of a state with two quarks are the symmetric and antisymmetric representations. For three quarks we have

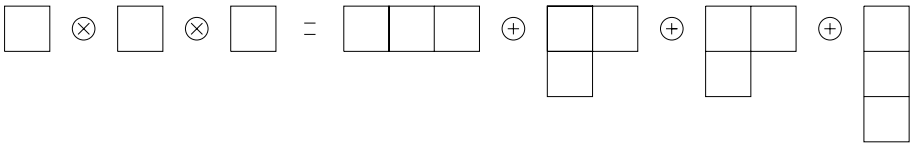

where in addition to the symmetric and antisymmetric representation there is a representation with mixed symmetry entering twice the decomposition.

The above results are the generalisation in SU(N) of the familiar decompositions in SU(3) $3 \otimes 3 = 6 \oplus \bar{3}$ and $3 \otimes 3 \otimes 3 = 10 \oplus 8 \oplus 8 \oplus 1$.

Once the symmetry of the states transforming under an irreducible representation has been worked out, it is easy to construct the operators implementing the transformation on such states, since those operators must have the same symmetry as the states on which they act. For the matrix elements of $k = 2$ operators associated to strings connecting sources with two quarks we obtain

$$A^{ij}_{lm} = \frac{1}{2}\left(U^i_l U^j_m - U^j_l U^i_m\right), \tag{40}$$

$$S^{ij}_{lm} = \frac{1}{2}\left(U^i_l U^j_m + U^j_l U^i_m\right), \tag{41}$$

while for $k = 3$ strings connecting three quarks we have

$$A^{ijk}_{lmn} = \frac{1}{6}\left(U^i_l U^j_m U^k_n - U^i_l U^k_m U^j_n - U^j_l U^i_m U^k_n + U^j_l U^k_m U^i_n + U^k_l U^i_m U^j_n - U^k_l U^j_m U^i_n\right), \tag{42}$$

$$S^{ijk}_{lmn} = \frac{1}{6}\left(U^i_l U^j_m U^k_n + U^i_l U^k_m U^j_n + U^j_l U^i_m U^k_n + U^j_l U^k_m U^i_n + U^k_l U^i_m U^j_n + U^k_l U^j_m U^i_n\right), \tag{43}$$

$$M^{ijk}_{lmn} = \frac{1}{3}\left(U^i_l U^j_m U^k_n - U^k_l U^j_m U^i_n + U^j_l U^i_m U^k_n - U^j_l U^k_m U^i_n\right), \tag{44}$$

A, S and M being respectively the tensors corresponding to the antisymmetric, the symmetric and one of the two mixed symmetry representations. (The other mixed symmetry representation has k and j interchanged in eqn(44).)

Taking the trace, we get

$$TrA = \frac{1}{2}\left(\{TrU\}^2 - TrU^2\right), \tag{45}$$

$$TrS = \frac{1}{2}\left(\{TrU\}^2 + TrU^2\right), \tag{46}$$

for k=2 and

$$TrA = \frac{1}{6}\left(\{TrU\}^3 - 3TrU\{TrU\}^2 + 2TrU^3\right), \quad (47)$$

$$TrS = \frac{1}{6}\left(\{TrU\}^3 + 3TrU\{TrU\}^2 + 2TrU^3\right), \quad (48)$$

$$TrM = \frac{1}{3}\left(\{TrU\}^3 - TrU^3\right), \quad (49)$$

for k=3. (The two different M's have the same trace.)

After identifying U with the path ordered product of links around a non-contractible loop c that winds once around the spatial torus, P_c, we get that the relevant operators for $k = 2$ are TrP_c^2 and $\{TrP_c\}^2$, while for $k = 3$ we will be concerned with TrP_c^3, $TrP_c\{TrP_c\}^2$ and $\{TrP_c\}^3$. These operators can be taken as a starting point for a variational procedure to extract the mass of flux tubes of $\mathcal{N}$-lity k winding once around the periodic lattice, while studying directly the combination corresponding to a given irreducible representation is relevant in the context of unstable strings (see the following Section).

The construction here explicitly provided for $k = 2$ and $k = 3$ can be easily generalised to any k.

A.2 Gluon screening

While in SU(N) gauge theories the $\mathcal{N}$-lity of a state is conserved by the dynamics, so isn't the representation: since the gluons transform under a non-trivial representation of SU(N), the interaction between them and the sources can change the original representation of the sources. In the group theoretical language, the product of this interaction transforms as the tensor product of the original representation and the adjoint representation. It is quite easy to see that this tensor product can be in a representation different from the original one. For instance, consider the following interaction:

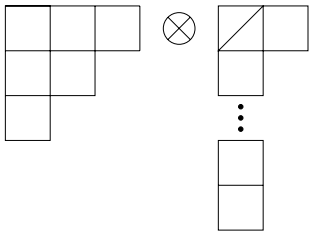

For simplicity, we will be concerned with the case where the number of quarks after interaction is still k. (This case is the only relevant at large N: since the dimension of a representation with $N+k$ quarks grows as N^{k+2}, while the dimension of a representation with k quarks is proportional to N^2, there is a phase-space suppression due to the

sudden lack of final states.) Such condition means that N boxes must be canceled (i.e. they are combined in such a way that they transform under the trivial representation). This can be done by taking an arbitrary box from the source and attaching it at the bottom of the first column of the gluon diagram, which is then reduced to a single box. The practical result of this procedure is that one box has been detached from the source. Such box can be then reattached anywhere, provided that the resulting diagram is a valid Young tableau.

Given the diagram of a source with m boxes in the first column, the cancellation of N boxes in the tensor product requires that $N - m$ boxes from the gluon are attached to the first column of the source. This can be done in two inequivalent ways: by taking the required objects all from rows other than the first one or by taking one box from the first row[2]. The possible ways of recombining the diagrams after the cancellation define the possible representations of the interacting state. Those representations depend on the original representation of the sources, but not on N.

The change of representation of the sources is expected to renormalise the string tension associated to the original representation. In addition, an interacting state will be energetically favourable whenever it has a smaller string tension, so we expect that the interaction tends to transform the sources in a given representation of $\mathcal{N}$-lity k to sources in the representation with the smallest string tension (which is the anti-symmetric representation with k quarks in both the Casimir scaling and the MQCD scenario), i.e. that the gluons screen the sources down to the states with the smallest string tension. However unstable strings are expected to be visible, since they should appear as nearly-stable excited states in the mass spectrum of the strings. Note that not all states with $\mathcal{N}$-lity k are accessible to a given state. For instance, the interaction with one gluon does not allow to pass from the symmetric to the antisymmetric representation at $k = 3$. However any state can be accessed by multiple interaction.

A.3 Quadratic Casimir operator and Casimir Scaling

The quadratic Casimir operator of a representation $\mathcal{R}$ is defined as

$$c_{\mathcal{R}} \equiv \sum_a T^a T^a \tag{50}$$

where the sum ranges over all the generators of the group in the given representation. It can be easily seen that the quadratic Casimir operator commutes with all the generators of the group. Hence, by virtue of the Schur's lemma, on a given representation it is proportional to the identity, i.e. it is identified by a number depending on the representation. We call such a number quadratic Casimir and we indicate it by $C_{\mathcal{R}}$. If we normalise the trace of the identity in each representation to 1, we can write

$$C_{\mathcal{R}} \equiv Tr T^a T^a. \tag{51}$$

[2]This argument should be refined if we were interested to the multiplicity with which each irreducible representation enters the decomposition of the tensor product.

$C_{\mathcal{R}}$ can be easily computed starting from the Young tableau associated to the representation $\mathcal{R}$ as follows. For SU(N), defines the N-dimensional vectors

$$\begin{aligned}
\vec{L}_1 &= \frac{1}{N}\,(N-1,-1,-1,-1,\ldots,-1)\,,\\
\vec{L}_2 &= \frac{1}{N}\,(N-2,N-2,-2,-2,\ldots,-2)\,,\\
\vec{L}_3 &= \frac{1}{N}\,(N-3,N-3,N-3,-3,\ldots,-3)\,,\\
&\vdots\\
\vec{L}_{N-1} &= \frac{1}{N}\,(1,1,1,,1,\ldots,-(N-1))\,,\\
2\vec{R} &= (N-1,N-3,N-5,\ldots,-(N-3),-(N-1))\,.
\end{aligned}$$

With the vectors $\vec{L}_i$, define

$$\vec{L} = \sum_{i=1}^{N-1} w_i L_i \tag{52}$$

where w_i is given by the difference between the number of boxes in the row i and the number of boxes in the row $i+1$ of the Young tableau. The quadratic Casimir is then given by

$$C_{\mathcal{R}} = \frac{1}{2}\left(\vec{L}\cdot\vec{L} + 2\vec{R}\cdot\vec{L}\right). \tag{53}$$

It is now easy to see that for an irreducible representation composed by k quarks the quadratic Casimir is given by the formula

$$C_{\mathcal{R}} = \frac{1}{2}\left(Nk + \sum_{i=1}^{m} n_i(n_i+1-2i) - \frac{k^2}{N}\right) \tag{54}$$

where i ranges over the rows of the Young tableau (with m number of rows) and n_i is the number of boxes in the i-th row. For the antisymmetric and the symmetric representations of $\mathcal{N}$-lity k we have

$$C_A = C_f \frac{k(N-K)}{N-1} \tag{55}$$

and

$$C_S = C_f \frac{k(N+K)}{N+1}, \tag{56}$$

$$C_f = \frac{N^2-1}{2N} \tag{57}$$

being the quadratic Casimir of the fundamental representation.

For $k = 3$ in addition to the symmetric and antisymmetric representations, there is (among others) the mixed symmetry representation, whose quadratic Casimir is

$$C_M = C_f \frac{3(N^2-3)}{N^2-1}. \tag{58}$$

Casimir scaling is the hypothesis that the string tension for a given representation is proportional to the quadratic Casimir. Hence, according to this hypothesis, at $\mathcal{N}$-lity k the smallest string tension is associated to sources in the representation with the smallest quadratic Casimir. By using eqn(54), it can be easily seen that the representation having the smallest quadratic Casimir is the antisymmetric representation composed by k quarks. To show this, let us prove as a preliminary step that at given number of quarks the totally antisymmetric representation has the lowest quadratic Casimir. Starting from an arbitrary representation, the difference between the quadratic Casimir of that representation and of the representation obtained by moving a box of the original Young diagram from the j-th row to the h-th row with $h > j$ is

$$\Delta C = n_j - n_h - 1 + j - h > 0. \tag{59}$$

It is now easy to prove the main statement: at given number of boxes $k \leq N/2$, the antisymmetric representation is obtained from any given representation by iterating the above procedure, with a series of steps where at each stage the quadratic Casimir decreases. Thus at given k the antisymmetric representation with k quarks has the smallest quadratic Casimir and for this reason the smallest string tension within the class of the representations with $\mathcal{N}$-lity k in the Casimir scaling hypothesis. This fact does old even if we consider states with $N + k$ quarks: the difference between the quadratic Casimir of the most antisymmetric representation with $N + k$ quarks (which is the smallest at that number of quarks) and the totally antisymmetric representation with k quarks is

$$\Delta C = N - k. \tag{60}$$

Not all the representations with k quarks have a larger quadratic Casimir than a given representation with $N + k$ quarks. For instance, the difference between the quadratic Casimir of the most antisymmetric representation with $N + k$ quarks and the totally symmetric representation with k quarks is

$$\Delta C = N - k^2, \tag{61}$$

which is negative if $k^2 > N$. However, at large enough N and at a given k such a difference is positive and increases as N. That is to say, we expect that the only relevant states of $\mathcal{N}$-lity k in the large N limit are those composed by k quarks.

The prediction of Casimir scaling for the ratio between the string tensions associated to states composed by $N + k$ quarks and the string tension of the fundamental representation in the limit $N \to \infty$ is $k + 2$. This result can be easily understood in terms

of string counting: a state with $N + k$ quarks can be seen as a possible state among those originated by the interaction between a state with k quarks and a gluon. The above result then tells us that at large N the energy of the composite state is equal to the sum of the energies of the constituents.

References

[1] M. Teper, Phys. Rev. D59 (1999) 014512 (hep-lat/9804008).

[2] A. Hanany, M. Strassler and A. Zaffaroni, Nucl. Phys. B513 (1998) 87 (hep-th/9707244).
M. Strassler, Nucl. Phys. Proc. Suppl. 73 (1999) 120 (hep-lat/9810059).
M. Strassler, Prog. Theor. Phys. Suppl. 131 (1998) 439 (hep-lat/9803009).

[3] J. Ambjorn, P. Olesen and C. Peterson, Nucl. Phys. B240 (1984) 189, 533; B244 (1984) 262; Phys. Lett. B142 (1984) 410.

[4] M. Lüscher, K. Symanzik and P. Weisz, Nucl. Phys. B173 (1980) 365.

[5] B. Lucini and M. Teper, Phys. Lett. B501 (2001) 128 (hep-lat/0012025).

[6] B. Lucini and M. Teper, hep-lat/0103027.

[7] J. Polchinski, *String Theory*, Vol I and II (CUP, 1998).

[8] P. Olesen, Phys. Lett. 160B (1985) 408.
M. Flensburg, A. Irbäck and C. Peterson, Z. Phys. C36 (1987) 629.
M. Caselle, R. Fiore, F. Gliozzi and R. Alzetta, Phys. Lett. 200B (1988) 525; 224B (1989) 153.
A. Loewy and J. Sonnenschein, hep-th/0103163.

[9] Ph. de Forcrand, G. Schierholz, H.Schneider and M. Teper, Phys. Lett. 160B (1985) 137.

[10] G. 't Hooft, Nucl. Phys. B72 (1974) 461.
E. Witten, Nucl. Phys. B160 (1979) 57.
S. Coleman, 1979 Erice Lectures.
A. Manohar, 1997 Les Houches Lectures, hep-ph/9802419.

[11] N. Cabibbo and E. Marinari, Phys. Lett. B119 (1982) 387.

[12] M. Teper, Phys. Lett. B183 (1987) 345.
M. Albanese et al (APE Collaboration), Phys. Lett. B192 (1987) 163.

[13] T. H. Hansson, Phys. Lett. B166 (1986) 343.

[14] K. Johnson and C. B. Thorn, Phys. Rev. D13 (1976) 1934.

[15] S. Deldar, Phys. Rev. D62 (2000) 034509 (hep-lat/9911008).

[16] G. Bali, Phys. Rev. D62 (2000) 114503 (hep-lat/0006022).

[17] S. Deldar, JHEP 0101 (2001) 013 (hep-ph/9912428).

[18] V. Shevchenko and Yu. Simonov, Phys. Rev. Lett. 85 (2000) 1811 (hep-ph/0001299); hep-ph/0104135 .

[19] Y. Koma, E.-M. Ilgenfritz, H. Toki and T. Suzuki, hep-ph/0103162.

[20] M. Wingate and S. Ohta, Phys. Rev. D63 (2001) 094502 (hep-lat/0006016).

[21] M. Creutz, *Quarks, gluons and lattices* (CUP 1983).
H. Rothe, *Lattice Gauge Theories* (World Scientific, 2nd Ed. 1997).
I. Montvay and G. Munster, *Quantum Fields on a Lattice* (CUP 1994).

[22] V. V. Schmidt, *The Physics of Superconductors* (Springer-Verlag, 1997).

[23] M. Teper, Phys. Lett. B311 (1993) 223.

[24] A. Hart, B. Lucini, Z. Schram and M. Teper, JHEP 0006 (2000) 040 (hep-lat/0005010).

[25] M. Teper, hep-th/9812187.

[26] M. Teper, Phys. Lett. B202 (1988) 553.

[27] P. Giovannangeli and C. Korthals Altes, hep-ph/0102022.

[28] G. 't Hooft, Nucl. Phys. B138 (1978) 1; B153 (1979) 141.

[29] A. Hart and M. Teper, Phys. Rev. D60 (1999) 114506 (hep-lat/9902031);
Phys. Rev. D58 (1998) 014504 (hep-lat/9712003).

[30] N. Isgur and J. Paton, Phys. Rev. D31 (1985) 2910.

[31] R. Johnson and M. Teper, hep-ph/0012287.

[32] L. Del Debbio, H. Panagopoulos, P. Rossi and E. Vicari, hep-th/0106185.

[33] H. F. Jones, *Groups, Representations and Physics* (Institute of Physics Publishing, 1996).
G. Racah, *Group Theory and Spectroscopy*, Ergebnisse der Exakten Naturwissenschaften vol. 37 (Springer-Verlag).

am_l ; SU(2) ; D=2+1				
lattice	MC sweeps	$p=0$	'safe' $p=0$	low p
$8^2 64$	4×10^5	0.1703(4)	0.1703(4)	0.1703(4)
$10^2 48$	8×10^5	0.2167(5)	0.2167(5)	0.2167(5)
$12^2 36$	10^6	0.2696(5)	0.2696(5)	0.2696(5)
$14^2 36$	2×10^6	0.3219(6)	0.3210(8)	0.3219(6)
$16^2 32$	2×10^6	0.3812(4)	0.3806(6)	0.3812(4)
$20^2 32$	2×10^6	0.4917(7)	0.4906(9)	0.4917(5)
$24^2 32$	2×10^6	0.5998(13)	0.5998(13)	0.6004(8)
$28^2 32$	2×10^6	0.7101(10)	0.7089(18)	0.7083(9)
$32^2 32$	2×10^6	0.8131(23)	0.8131(23)	0.8150(15)
$36^2 32$	2×10^6	0.9175(33)	0.9167(38)	0.9195(19)
$40^2 32$	2×10^6	1.0238(53)	1.0238(53)	1.0284(24)

Table 1: The lightest mass am_l of a fundamental string wrapped around a spatial torus. The first column comes from good fits to $p=0$ correlators, chosen so as to minimise the errors. The second column contains cautious 'very safe' estimates with larger errors. The third column uses both $p=0$ and, where useful, $p\neq0$ correlators.

$c_s^{eff}(l,l')$; SU(2) ; D=2+1				
L	L'	$p=0$	'safe' $p=0$	low p
8	10	0.130(24)	0.130(24)	0.130(24)
10	12	0.498(41)	0.498(41)	0.498(41)
12	14	0.546(62)	0.479(73)	0.546(62)
14	16	1.329(79)	1.37(11)	1.329(79)
16	20	1.046(58)	1.01(8)	1.032(48)
20	24	0.99(16)	1.15(18)	1.08(10)
24	28	1.53(27)	1.35(35)	1.16(19)
28	32	0.31(51)	0.6(6)	1.10(36)
32	36	0.7(1.1)	0.5(1.2)	0.68(66)
36	40	1.4(2.1)	1.7(2.2)	2.2(1.0)

Table 2: Estimating the effective string correction coefficient from the masses of pairs of flux loops of length $l=aL$ and $l'=aL'$ respectively, using eqn(10).

$c_s(l \geq l_0)$; SU(2) ; D=2+1						
L_0	$p=0$	χ^2/dof	'safe' $p=0$	χ^2/dof	low p	χ^2/dof
14	–	–	1.12(6)	1.3	1.10(3)	1.6
16	1.07(5)	1.2	1.07(8)	0.4	1.070(45)	0.4
20	1.09(10)	1.4	1.11(15)	0.5	1.11(9)	0.3
24	1.02(25)	1.9	1.01(25)	0.5	1.12(15)	0.4
28	0.52(40)	0.2	0.7(6)	0.1	1.10(24)	0.6
32	0.9(8)	0.1	–	–	1.2(5)	1.0

Table 3: Estimating the string correction coefficient from a fit of eqn(6) to the masses of all the flux loops of length $l \geq l_0 = aL_0$. In each case we show the χ^2/dof of the best fit.

am_l ; SU(2) ; D=3+1					
lattice	MC sweeps	$p=0$	'safe' $p=0$	low p	'safe' low p
$10^3 60$	10^5	0.1679(14)	0.1679(14)	0.1679(14)	0.1679(14)
$12^3 48$	2×10^5	0.2073(14)	0.2073(14)	0.2073(14)	0.2073(14)
$14^3 36$	4×10^5	0.2632(13)	0.2606(16)	0.2636(12)	0.2606(16)
$16^3 28$	6×10^5	0.3230(18)	0.3230(18)	0.3302(11)	0.3230(18)
20^4	6×10^5	0.4468(15)	0.4416(23)	0.4408(20)	0.4408(20)
24^4	8×10^5	0.5476(22)	0.5476(22)	0.5459(15)	0.5459(15)
$32^3 24$	4×10^5	0.7598(75)	0.7469(115)	0.7549(50)	0.7496(58)

Table 4: The lightest mass am_l of a fundamental string wrapped around a spatial torus. The first column comes from good fits to $p = 0$ correlators, chosen so as to minimise the errors. The second column contains cautious 'very safe' estimates with larger errors. The third and fourth columns use both $p = 0$ and, where useful, $p \neq 0$ correlators.

$c_s^{eff}(l, l')$; SU(2) ; D=3+1					
L	L'	$p=0$	'safe' $p=0$	low p	'safe' low p
10	12	0.15(6)	0.15(6)	0.15(6)	0.15(6)
12	14	0.79(8)	0.69(9)	0.81(8)	0.69(9)
14	16	1.11(12)	1.26(13)	1.44(9)	1.26(13)
16	20	1.46(9)	1.28(11)	0.95(8)	1.26(10)
20	24	0.60(15)	0.92(18)	0.88(15)	0.88(15)
24	32	1.17(32)	0.66(47)	1.06(21)	0.85(24)

Table 5: Estimating the effective string correction coefficient from the masses of pairs of flux loops of length $l = aL$ and $l' = aL'$ respectively, using eqn(10).

$c_s(l \geq l_0)$; SU(2) ; D=3+1						
L_0	'safe' $p = 0$	χ^2/dof	low p	χ^2/dof	'safe' low p	χ^2/dof
14	1.19(7)	1.5	–	–	1.15(7)	2.2
16	1.14(12)	1.7	0.94(6)	0.2	1.09(9)	2.2
20	0.88(20)	0.2	0.95(14)	0.4	0.87(13)	0.0

Table 6: Estimating the string correction coefficient from a fit of eqn(6) to the masses of all the flux loops of length $l \geq l_0 = aL_0$. In each case we show the χ^2/dof of the best fit.

D=3+1			
SU(4)		SU(5)	
β	$a\sqrt{\sigma}$	β	$a\sqrt{\sigma}$
10.55	0.372	16.755	0.384
10.70	0.306	16.975	0.303
10.90	0.243	17.270	0.245
11.10	0.202	17.450	0.222
11.30	0.170	–	–

Table 7: Setting the scale of a: the string tension for our SU(4) and SU(5) lattice calculations in D=3+1.

D=3+1 ; SU(4)				
β	lattice	MC sweeps	$am_{k=1}$	$am_{k=2}$
10.55	8^4	2×10^5	0.973(17)	1.456(30)
10.70	$6^3 16$	5×10^4	0.268(8)	0.329(12)
10.70	$8^3 12$	10^5	0.564(10)	0.763(24)
10.70	10^4	10^5	0.8375(92)	1.197(18)
10.70	12^4	10^5	1.033(11)	1.456(37)
10.70	14^4	10^5	1.201(34)	1.780(60)
10.70	16^4	10^5	1.316(78)	2.35(27)
10.90	12^4	10^5	0.622(7)	0.896(11)
11.10	16^4	10^5	0.585(8)	0.836(21)
11.30	20^4	10^5	0.5265(56)	0.740(16)

Table 8: Masses of the $k = 1$ and $k = 2$ flux loops that wind once around the spatial torus. In D=3+1 SU(4), for the lattices and couplings shown.

D=3+1 ; SU(5)				
β	lattice	MC sweeps	$am_{k=1}$	$am_{k=2}$
16.755	8^4	10^5	1.051(13)	1.70(7)
16.975	10^4	2.0×10^5	0.816(12)	1.239(51)
17.270	12^4	1.4×10^5	0.638(9)	1.061(28)
17.450	16^4	10^5	0.723(10)	1.168(62)

Table 9: Masses of the $k = 1$ and $k = 2$ flux loops that wind once around the spatial torus. In D=3+1 SU(5), for the lattices and couplings shown.

D=2+1			
SU(4)		SU(6)	
β	$a\sqrt{\sigma}$	β	$a\sqrt{\sigma}$
18.0	0.442	42.0	0.436
21.0	0.361	49.0	0.353
28.0	0.252	60.0	0.274
33.0	0.208	75.0	0.211
45.0	0.147	108.0	0.141
60.0	0.108	–	–

Table 10: Setting the scale of a: the string tension for our SU(4) and SU(6) lattice calculations in D=2+1.

D=2+1 ; SU(4)				
β	lattice	MC sweeps	$am_{k=1}$	$am_{k=2}$
18.0	8^3	2×10^5	1.497(18)	2.022(66)
21.0	10^3	2×10^5	1.223(11)	1.690(38)
28.0	$4^2 48$	10^5	0.1347(12)	0.1836(21)
28.0	$6^2 28$	10^5	0.2724(15)	0.3630(26)
28.0	$8^2 16$	10^5	0.4276(33)	0.5652(64)
28.0	$10^2 16$	1.5×10^5	0.5720(30)	0.7824(63)
28.0	12^3	2×10^5	0.7152(39)	0.9718(95)
28.0	16^3	2×10^5	0.9937(58)	1.345(14)
33.0	16^3	2×10^5	0.6622(29)	0.914(6)
45.0	24^3	2×10^5	0.4974(22)	0.6815(40)
60.0	32^3	2×10^5	0.3571(14)	0.4888(15)

Table 11: Masses of the $k = 1$ and $k = 2$ flux loops that wind once around the spatial torus. In D=2+1 SU(4), for the lattices and couplings shown.

D=2+1 ; SU(6)					
β	lattice	MC sweeps	$am_{k=1}$	$am_{k=2}$	$am_{k=3}$
42.0	8^3	3×10^5	1.453(14)	2.51(10)	2.85(30)
49.0	10^3	2×10^5	1.194(9)	2.030(42)	2.21(9)
60.0	12^3	2×10^5	0.8575(47)	1.443(15)	1.621(25)
75.0	16^3	2×10^5	0.6825(31)	1.1305(72)	1.275(11)
108.0	24^3	3×10^5	0.4552(13)	0.7534(21)	0.8424(98)

Table 12: Masses of the $k = 1$, $k = 2$ and $k = 3$ flux loops that wind once around the spatial torus. In D=2+1 SU(6), for the lattices and couplings shown.

D=2+1 ; SU(4) ; $\beta = 28$				
	$am_{k=1}(L)$		$am_{k=2}(L)$	
$L_\perp$	$L = 8$	$L = 12$	$L = 8$	$L = 12$
2	1.188(10)	1.811(23)	1.552(28)	2.27(10)
3	0.738(9)	1.1900(73)	1.008(11)	1.45(15)
4	0.5093(37)	0.819(13)	0.667(9)	1.04(4)
5	0.4297(36)	0.6814(83)	0.5583(62)	0.899(12)
6	0.4207(28)	0.6965(46)	0.5504(57)	0.869(22)
8	0.4276(33)	0.710(5)	0.5652(64)	0.947(9)
10	0.4274(30)	0.706(5)	0.5770(56)	0.971(11)
12	0.4327(30)	0.715(4)	0.5985(58)	0.972(10)
16	0.4347(28)	0.721(5)	0.598(7)	0.948(24)
20	0.4331(30)	0.713(4)	0.600(5)	0.991(12)

Table 13: Masses of flux loops that wind once around a spatial torus of length L, as a function of the length, $L_\perp$, of the other spatial torus.

D=2+1 ; SU(6) ; $\beta = 60$						
	$am_{k=1}(L)$		$am_{k=2}(L)$		$am_{k=3}(L)$	
$l_\perp$	$L = 10$	$L = 12$	$L = 10$	$L = 12$	$L = 10$	$L = 12$
2	1.40(13)	2.055(8)	2.66(20)	2.70(41)	3.11(4)	2.63(91)
3	1.050(29)	1.227(56)	1.785(38)	2.069(51)	1.929(70)	2.33(21)
4	0.692(12)	0.841(18)	1.178(14)	1.419(28)	1.360(27)	1.611(54)
5	0.6767(66)	0.8455(65)	1.064(14)	1.280(11)	1.163(16)	1.389(31)
6	0.6915(67)	0.8462(59)	1.084(12)	1.368(23)	1.200(21)	1.531(31)
8	0.7005(52)	0.8671(54)	1.137(14)	1.390(23)	1.194(65)	1.590(37)
10	0.7015(49)	0.843(13)	1.180(14)	1.435(16)	1.327(27)	1.658(55)
12	–	0.8575(47)	–	1.443(15)	–	1.621(25)

Table 14: Masses of flux loops that wind once around a spatial torus of length L, as a function of the length, $L_\perp$, of the other spatial torus.

D=3+1 ; SU(4) ; finite T				
L_t	$T/\sqrt{\sigma}$	$\langle l_p \rangle$	am_t	$\langle Q^2 \rangle$
2	1.63	0.5669(1)	0.000	–
3	1.09	0.3414(1)	0.003	–
4	0.82	0.1922(2)	0.005	0.002(1)
5	0.65	0.0041(40)	0.052(1)	0.150(15)
6	0.54	-0.0006(10)	0.230(8)	1.363(53)
10	'0.33'	–	0.838(9)	2.56(9)

Table 15: Calculations at finite temperature, T, on $10^3 \times L_t$ lattices. In SU(4) at $\beta = 10.7$. We show the thermal line average, $\langle l_p \rangle$, the lightest mass coupled to the thermal line, am_t, and the size of the topological fluctuations, $\langle Q^2 \rangle$.

D=3+1 ; SU(4) ; finite T				
			$\sigma_{k=2}/\sigma$	
L_t	$am_{k=1}$	$am_{k=2}$	$c_s = 0$	$c_s = 1$
2	2.71(17)	2.7(7)	–	–
3	1.523(28)	2.11(10)	1.385(70)	1.361(66)
4	1.044(9)	1.40(3)	1.341(30)	1.310(28)
5	0.800(9)	1.101(20)	1.376(30)	1.333(26)
6	0.727(16)	0.90(4)	1.238(55)	1.208(54)
10	0.838(9)	1.197(18)	1.429(27)	1.382(23)

Table 16: Calculations at the finite temperatures listed in Table 15. We list the 'spatial' loop masses and the corresponding ratio of 'spatial' string tensions, calculated with and without a bosonic string correction.

D=2+1 ; SU(4)		
β	lattice	$am_{k=2S}$
28.0	12^3	1.601(23)
33.0	16^3	1.352(15)
45.0	24^3	0.979(40)
60.0	32^3	0.7694(70)

Table 17: Masses of flux loops in the $k = 2$ symmetric representation. In D=2+1 SU(4), for the lattices and couplings shown.

D=2+1 ; SU(6)				
β	lattice	$am_{k=2S}$	$am_{k=3M}$	$am_{k=3S}$
49.0	10^3	2.58(19)	–	–
60.0	12^3	1.928(41)	2.44(12)	–
75.0	16^3	1.512(15)	1.845(37)	2.270(87)
108.0	24^3	1.015(12)	1.0210(47)	1.015(12)

Table 18: Masses of flux loops in the $k = 2$ symmetric ($k = 2S$), $k = 3$ mixed ($k = 3M$) and $k = 3$ symmetric ($k = 3S$) representations. In D=2+1 SU(6), for the lattices and couplings shown.

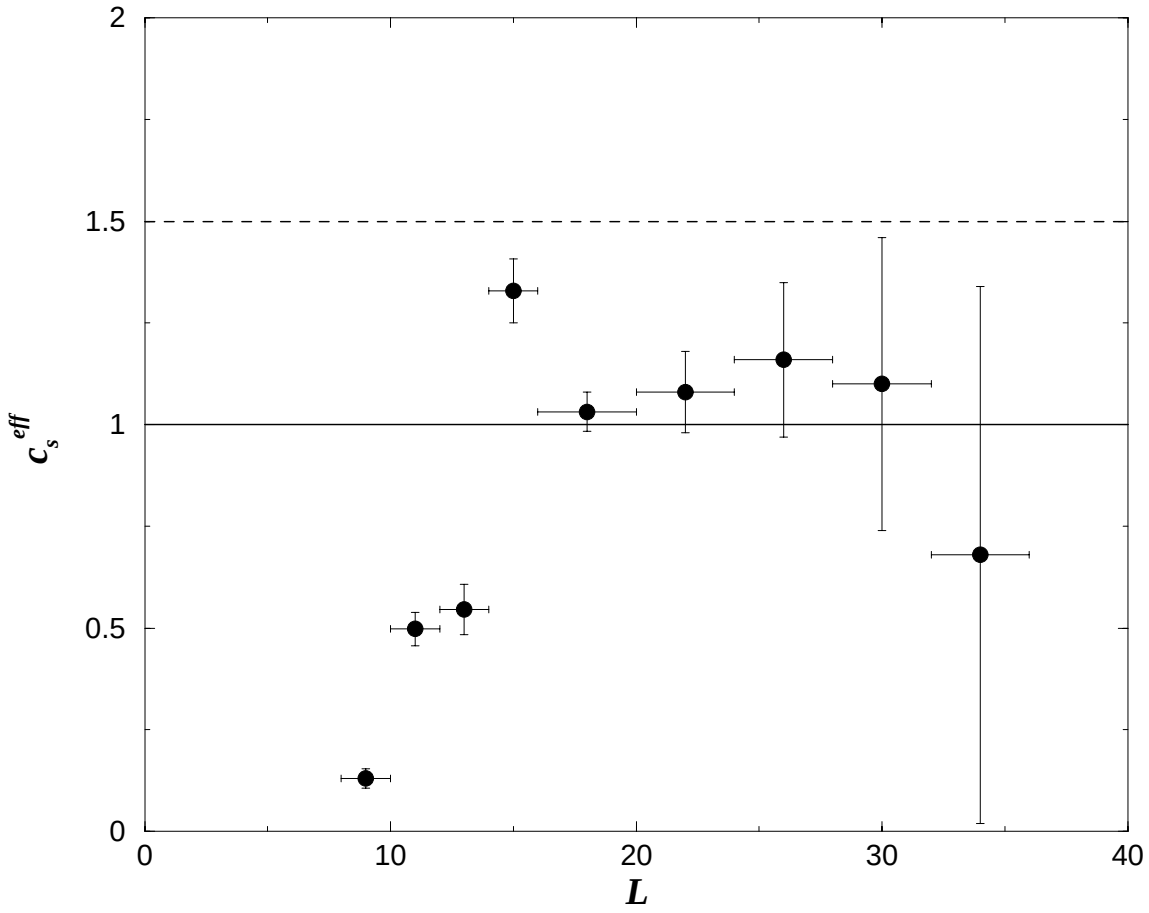

Figure 1: The D=2+1 effective string correction coefficient estimated from the masses of flux loops of different lengths (indicated by the span of the horizontal error bar) using eqn(10). The solid line is what one expects for a simple bosonic string. For comparison the dashed line indicates the value for the Neveu-Schwartz string.

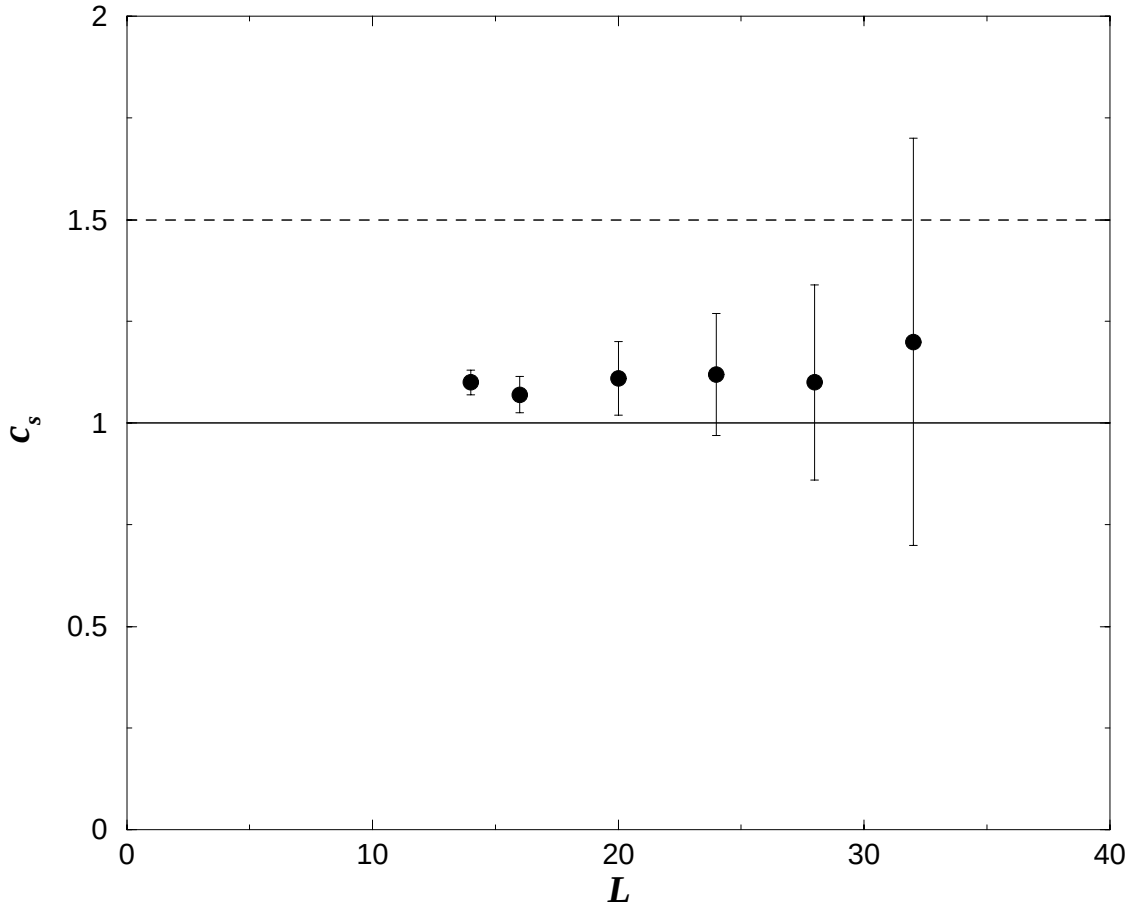

Figure 2: The D=2+1 string correction coefficient estimated by fitting the masses of all flux loops with length greater than L, as a function of L.

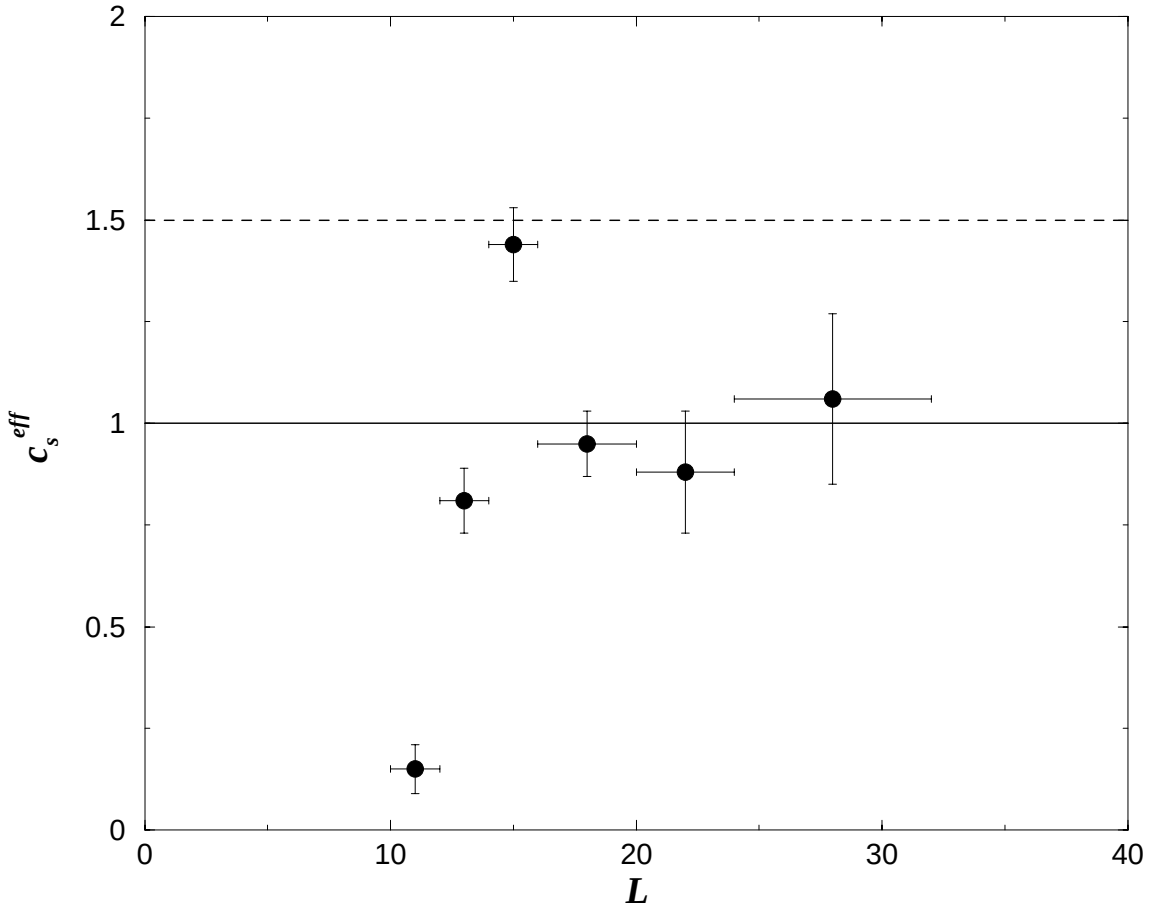

Figure 3: The D=3+1 effective string correction coefficient estimated from the masses of flux loops of different lengths (indicated by the span of the horizontal error bar) using eqn(10). The solid line is what one expects for a simple bosonic string. For comparison dashed line indicates the value for the Neveu-Schwartz string. We use masses from the third column in Table 5.

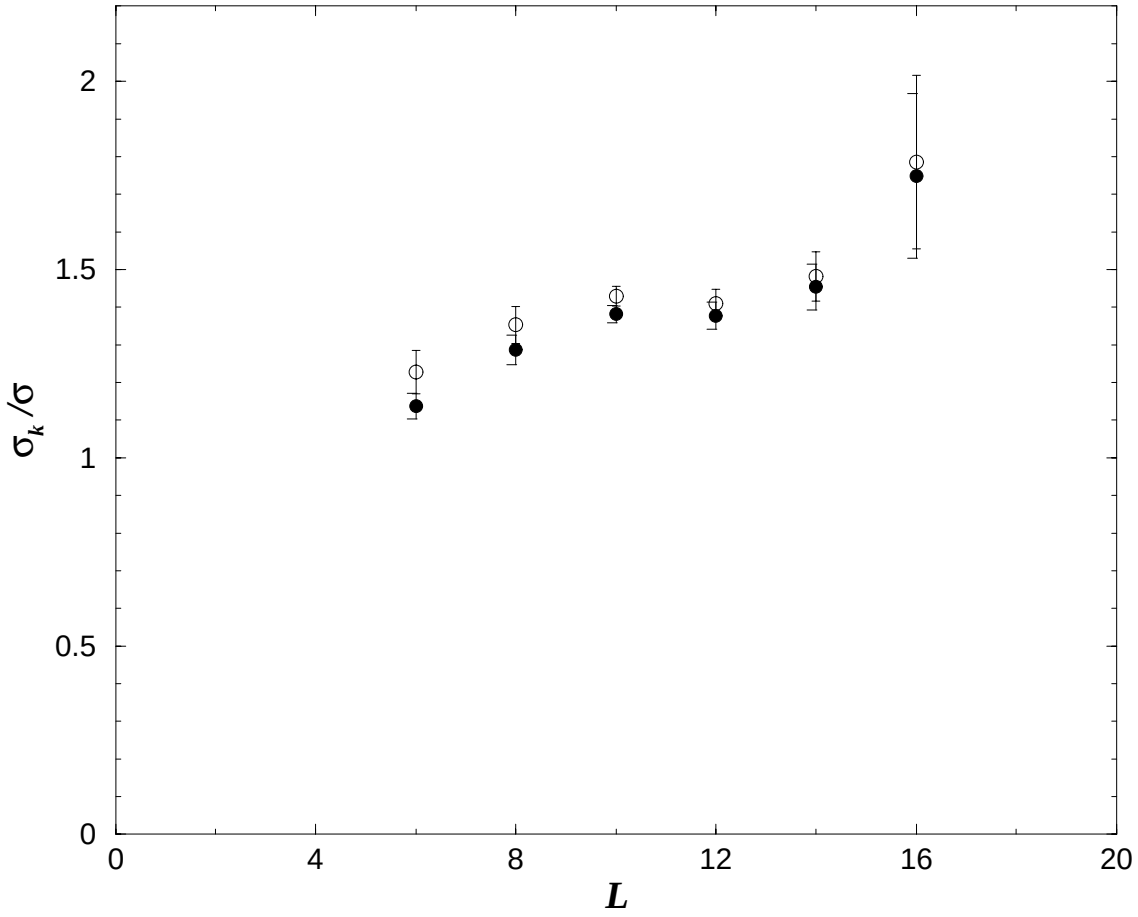

Figure 4: The ratio of $k = 2$ and $k = 1$ string tensions in D=3+1 SU(4) at $\beta = 10.7$ extracted from flux loops of length $l = aL$. We show values extracted using a bosonic string correction, (•), and no string correction at all (∘).

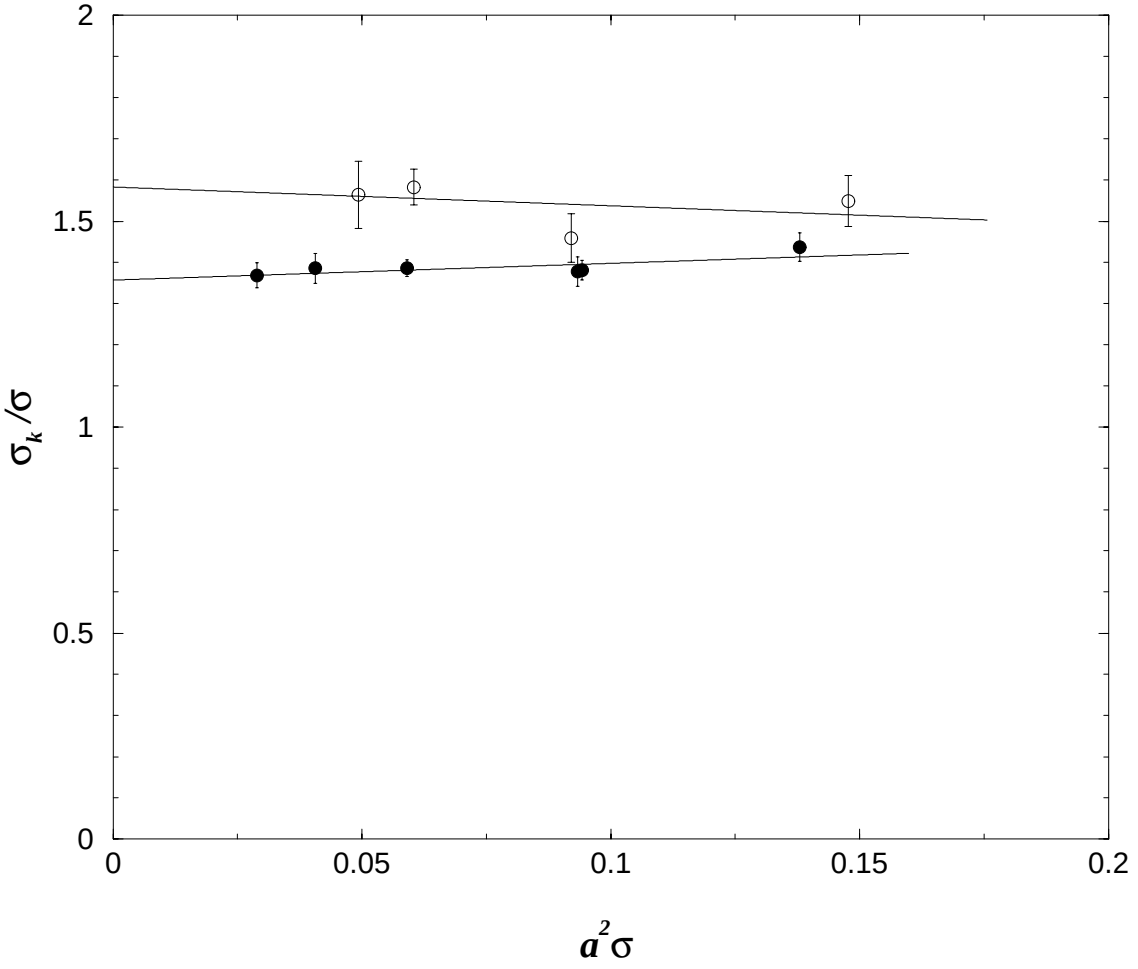

Figure 5: The ratio of $k = 2$ and $k = 1$ string tensions in our D=3+1 SU(4) ($\bullet$) and SU(5) ($\circ$) lattice calculations plotted as a function of $a^2\sigma$. Extrapolations to the continuum limit, using a leading $O(a^2)$ correction, are displayed.

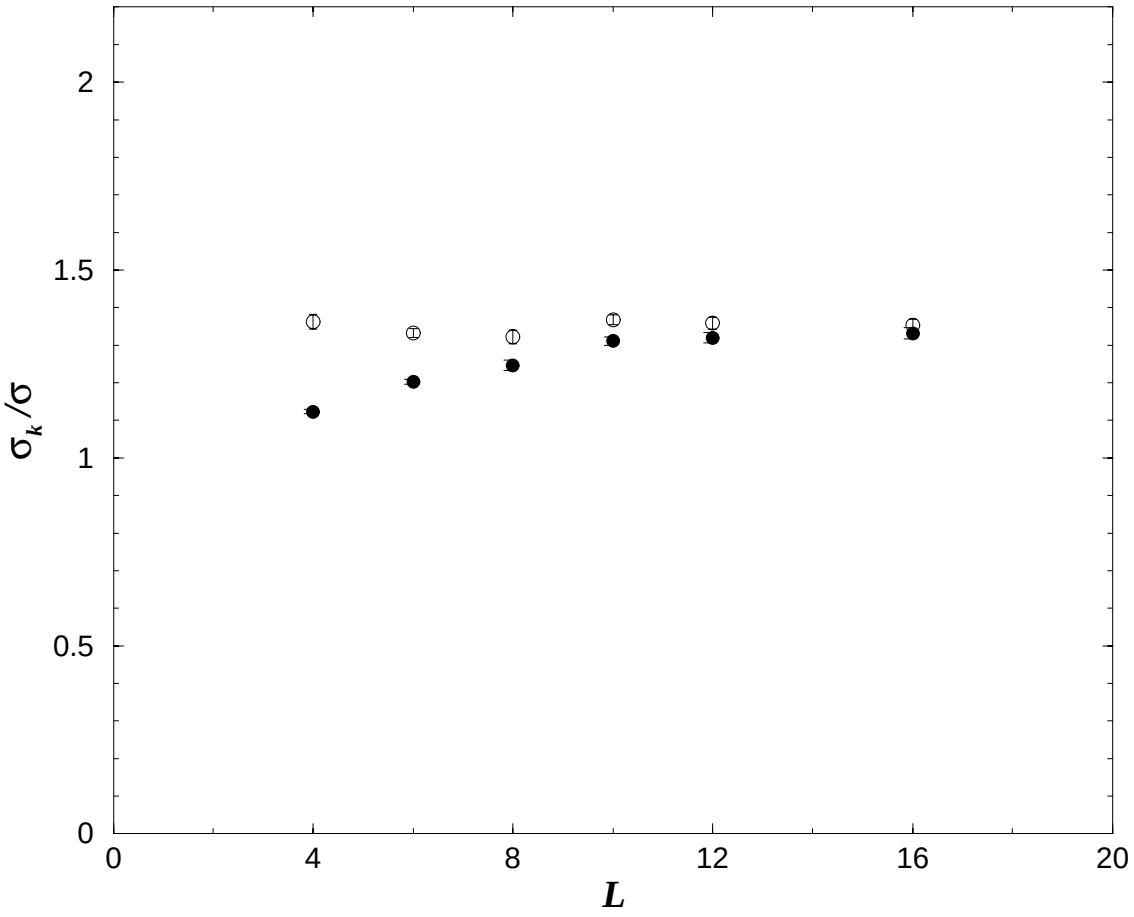

Figure 6: The ratio of $k = 2$ and $k = 1$ string tensions in D=2+1 SU(4) at $\beta = 28.0$ extracted from flux loops of length $l = aL$. We show values extracted using a bosonic string correction, (•), and no string correction at all (∘).

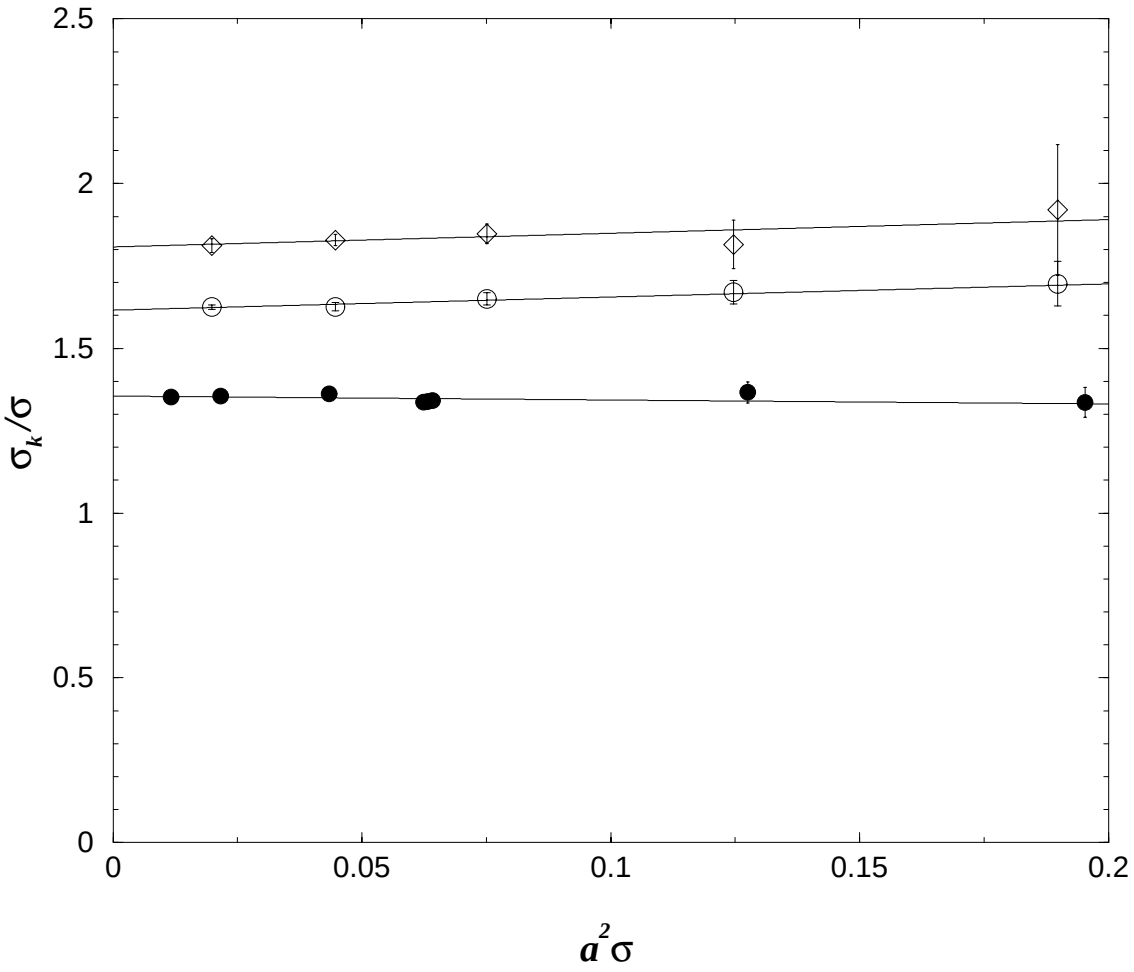

Figure 7: The ratio of $k = 2$ and $k = 1$ string tensions in our D=2+1 SU(4) ($\bullet$) and SU(6) ($\circ$) lattice calculations plotted as a function of $a^2\sigma$. Also shown is the $k = 3$ to $k = 1$ ratio ($\diamond$) in SU(6). Extrapolations to the continuum limit, using a leading $O(a^2)$ correction, are displayed.

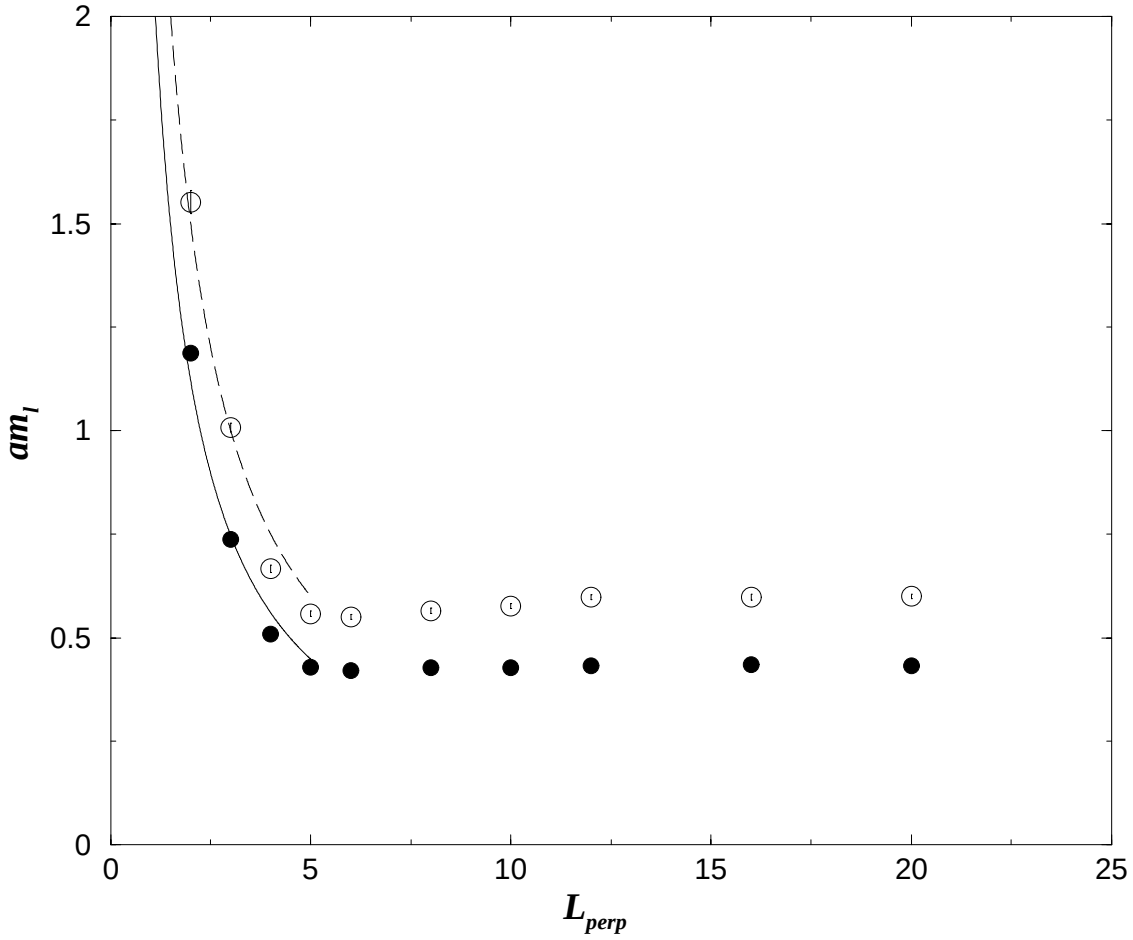

Figure 8: The masses of the $k = 1$ and $k = 2$ flux loops of length $L = 8$ in the D=2+1 SU(4) gauge theory at $\beta = 28$, versus the size of the transverse spatial torus $L_{perp} \equiv L_\perp$. Shown is the dependence in eqn(31) fitted to the smallest values of L_{perp}.

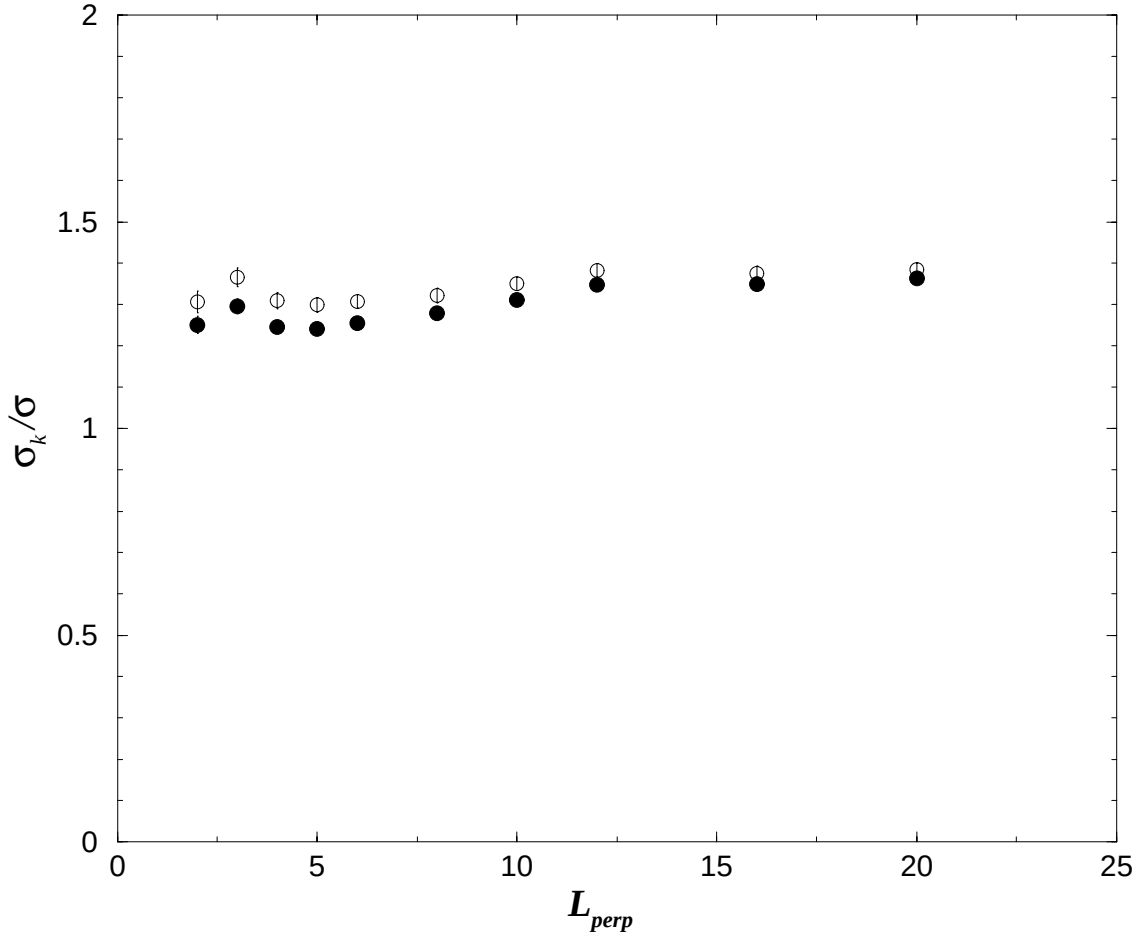

Figure 9: The ratio of the $k = 2$ to $k = 1$ string tensions in the D=2+1 SU(4) gauge theory at $\beta = 28$ versus the size of the transverse spatial torus $L_{perp} \equiv L_\perp$. With ($\bullet$) and without ($\circ$) a (bosonic) string correction.

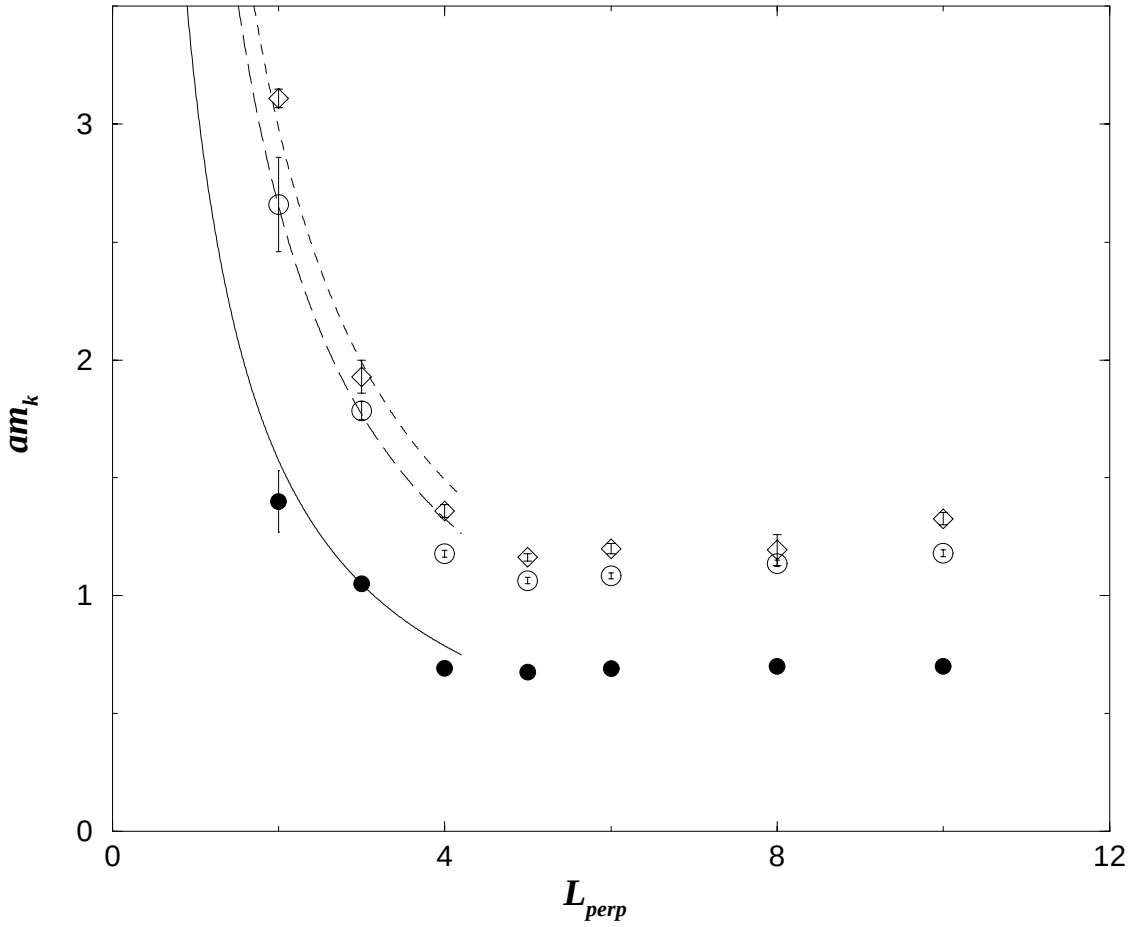

Figure 10: The masses of the $k = 1$, $k = 2$ and $k = 3$ flux loops of length $L = 10$ in the D=2+1 SU(6) gauge theory at $\beta = 60$ versus the size of the transverse spatial torus $L_{perp} \equiv L_\perp$. Shown is the dependence in eqn(31) fitted to the smallest values of L_{perp}.

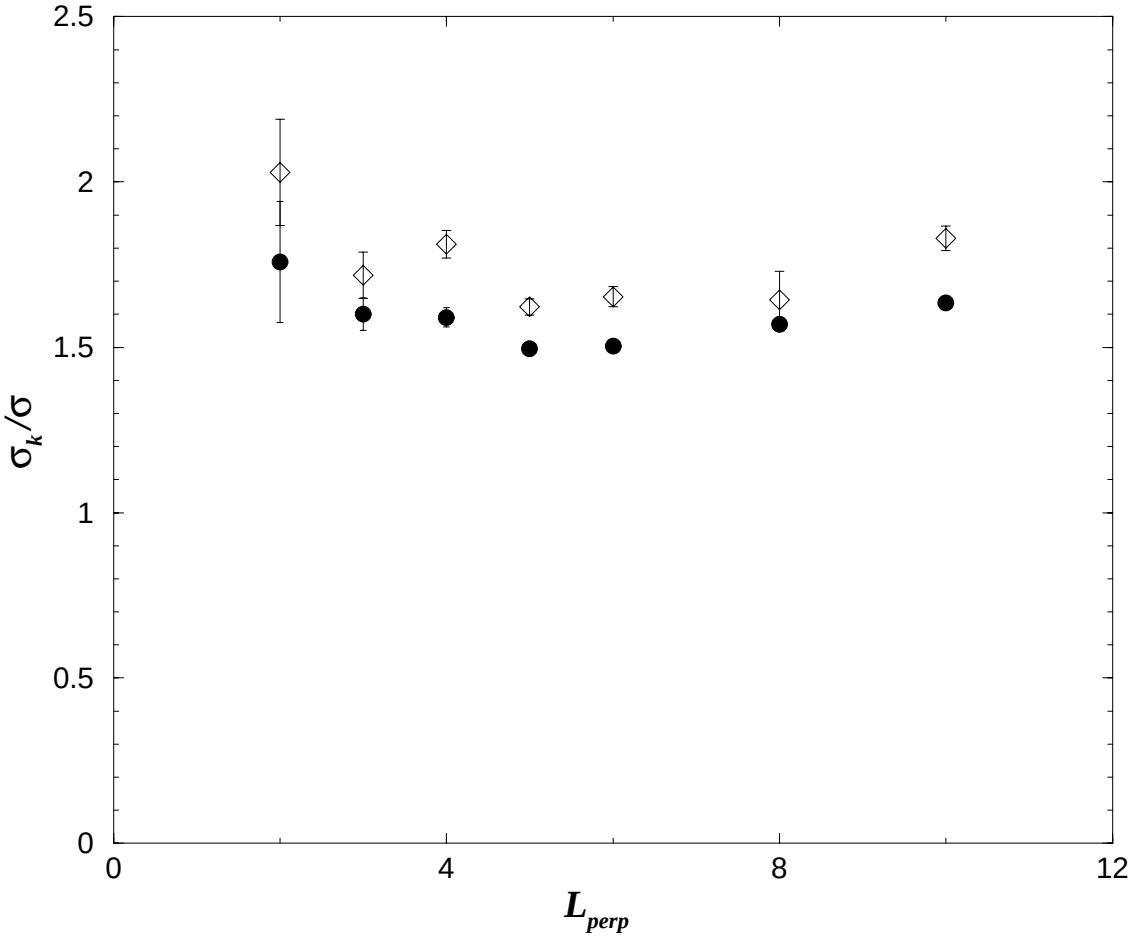

Figure 11: The ratio of the $k = 2$ to $k = 1$ ($\bullet$) and $k = 3$ to $k = 1$ ($\diamond$) string tensions in the D=2+1 SU(6) gauge theory at $\beta = 60$ versus the size of the transverse spatial torus $L_{perp} \equiv L_\perp$. The (bosonic) string correction has been included.